Research Article

Nano Research
2023, 16(2): 3536–3541

ISSN 1998-0124 CN 11-5974/O4
https://doi.org/10.1007/s12274-022-4996-9

Efficient capture of C_2H_2 from CO_2 and C_nH_4 by a novel fluorinated anion pillared MOF with flexible molecular sieving effect

Lingyao Wang[1], Nuo Xu[1], Yongqi Hu[1], Wanqi Sun[1], Rajamani Krishna[2], Jiahao Li[1], Yunjia Jiang[1], Simon Duttwyler[3], and Yuanbin Zhang[1] (✉)

[1] *Key Laboratory of the Ministry of Education for Advanced Catalysis Materials, College of Chemistry and Life Sciences, Zhejiang Normal University, Jinhua 321004, China*
[2] *Van't Hoff Institute for Molecular Sciences, University of Amsterdam, Science Park 904, Amsterdam 1098 XH, the Netherlands*
[3] *Department of Chemistry, Zhejiang University, Hangzhou 310027, China*

Received: 12 July 2022 / **Revised:** 11 August 2022 / **Accepted:** 31 August 2022

ABSTRACT

The efficient separation of acetylene (C_2H_2) from carbon dioxide (CO_2) and C_nH_4 (n = 1 and 2) to manufacture high purity C_2H_2 and recover other light hydrocarbons is technologically important, while posing significant challenges. Herein, we reported a new TiF_6^{2-} anion (TIFSIX) pillared metal-organic framework (MOF) ZNU-5 (ZNU = Zhejiang Normal University) with ultramicropores for highly selective C_2H_2 capture with low adsorption heat through gate opening based molecular sieving effect. ZNU-5 takes up a large amount of C_2H_2 (128.6 cm^3/g) at 1.0 bar and 298 K but excludes CO_2, CH_4, and C_2H_4. Such high capacity has never been realized in MOFs with molecular sieving. The breakthrough experiments further confirmed the highly selective C_2H_2 separation performance from multi-component gas mixtures. 3.3, 2.8, and 2.2 mmol/g of C_2H_2 is captured at ZNU-5 from equimolar C_2H_2/CO_2, $C_2H_2/CO_2/CH_4$, and $C_2H_2/CO_2/CH_4/C_2H_4$ mixtures, respectively. Furthermore, 2.6, 2.0, and 1.5 mmol/g of > 98% purity C_2H_2 can be recycled from the desorption process. Combining high working capacity, low adsorption heat, as well as good recyclability, ZNU-5 is promising for C_2H_2 purification.

KEYWORDS

metal-organic frameworks (MOFs), C_2H_2/CO_2 separation, acetylene recovery, molecular sieving, flexible MOFs

1 Introduction

Acetylene (C_2H_2) is a major raw feedstock for the production of various essential chemicals and polymers in industry [1–3]. It is produced from the partial combustion of natural gas or stream cracking of hydrocarbons, in which carbon dioxide (CO_2) and other C_1-C_2 light hydrocarbons are worth-noting contaminants that need to be removed to produce C_2H_2 in high purity [4, 5]. Currently, energy-intensive cryogenic distillation and solvent extraction are employed for the recovery of C_2H_2 from other gases. Due to the close boiling points, these approaches suffer from low energy inefficiency and are environmentally unfriendly. Therefore, physisorptive separation using porous solid adsorbents has attracted particular interest based on the lower cost and energy consumption [6–16]. However, the similarities among these gas molecules in terms of molecular size (kinetic diameter: 3.3 Å for both C_2H_2 and CO_2, 3.8 Å for CH_4, and 4.2 Å for C_2H_4) and physical properties make these separations a great challenge [17–21].

Metal-organic frameworks (MOFs) are famous for their powerful structural predictability and tunability on pore size/shape and functionality [22–30]. However, the flexibility of MOFs is still very challenging to predict and flexible MOFs have less been studied in selective gas separation. UTSA-300 (SIFSIX-dps-Zn; SIFSIX = SiF_6^{2-}, dps = 4,4′ -dipyridylsulfide) [31] is the first reported flexible MOF that takes up 69.0 cm^3/g of C_2H_2 and negligible CO_2 and C_2H_4. By replacing the zinc ion (Zn^{2+}) to copper ion (Cu^{2+}), the resulting SIFSIX-dps-Cu [32] exhibits increased C_2H_2 uptake of 102.4 cm^3/g as well as an ultrahigh selectivity of 1,787. However, the practical dynamic capacity of C_2H_2 from equimolar C_2H_2/CO_2 mixture is only 2.48 mmol/g, even lower than that (2.9 mmol/g) of our recently reported robust MOF ZNU-1 (ZNU = Zhejiang Normal University) [33] with static uptake of 76.3 cm^3/g and ideal adsorbed solution theory (IAST) selectivity of 56.6. Therefore, high practical working capacity is still very difficult to realize by flexible MOFs in the context of challenging C_2H_2/CO_2 separation.

Herein, we would like to report a new TiF_6^{2-} anion (TIFSIX) pillared flexible metal-organic framework ZNU-5 for selective C_2H_2 adsorption. ZNU-5 is constructed by self-assembly of $CuTiF_6$ and 1,4-di(1H-imidazol-1-yl)benzene (DIB) in $MeOH/H_2O$ solution. It displays a large capacity of 128.6 cm^3/g for C_2H_2 under 1.0 bar and 298 K but only adsorbs 15.2, 11.9, and 3.5 cm^3/g of CO_2, C_2H_4, and CH_4. The near-zero coverage C_2H_2 adsorption heat is as low as 27.8 kJ/mol, indicative of its low energy footprint for material regeneration. The calculated IAST selectivities at 1.0 bar are 11.6 for C_2H_2/CO_2, 255 for C_2H_2/C_2H_4, and 850 for C_2H_2/CH_4. Such high selectivities have rarely been achieved by reported top-performing MOFs. The practical separation performance is fully demonstrated by the breakthrough

Address correspondence to ybzhang@zjnu.edu.cn

experiments of multi-component gas mixtures. 3.3, 2.8, and 2.2 mmol/g of C_2H_2 is captured at ZNU-5 from 50/50 C_2H_2/CO_2, 33.3/33.3/33.3 $C_2H_2/CO_2/CH_4$, and 25/25/25/25 $C_2H_2/CO_2/CH_4/C_2H_4$ mixtures, respectively. 2.6, 2.0, and 1.5 mmol/g of > 98% purity C_2H_2 can be recycled from the desorption process. No separation performance reduction is observed over 5 cycles. Therefore, combining high working capacity, low adsorption heat, as well as good recyclability, ZNU-5 is promising for C_2H_2 purification.

2 Experimental

2.1 Synthesis of ZNU-5

To a 5 mL long thin tube was added 1 mL of aqueous solution with $(NH_4)_2TiF_6$ (1 mg) and $Cu(NO_3)_2{\cdot}3H_2O$ (1 mg). 3 mL of MeOH/H_2O mixture was slowly layered above the solution, followed by 1 mL of MeOH solution of 1,4-di(1H-imidazol-1-yl)benzene (2 mg). The tube was sealed and left undisturbed at room temperature. After several days, purple needle-shaped crystals were formed on the glass surface. The average yield was ca. 75%.

2.2 Synthesis of ZNU-4

To a 5 mL long thin tube was added 1 mL of aqueous solution with $(NH_4)_2TiF_6$ (1 mg) and $Cu(NO_3)_2{\cdot}3H_2O$ (1 mg). 2 mL of MeCN/H_2O mixture was slowly layered above the solution, followed by 1 mL of MeCN solution of 1,4-di(1H-imidazol-1-yl)benzene (2 mg). The tube was sealed and left undisturbed at room temperature. After several days, blue flake shaped crystals were formed on the glass surface. The average yield was ca. 75%.

3 Results and discussion

3.1 Structural analysis and characterization

Light blue single crystals of ZNU-4 [34] with zsd topology was prepared in MeCN/H_2O solution (Fig. S2(a) in the Electronic Supplementary Material (ESM)). Each Cu(II) ion of ZNU-4 is connected to four imidazole nitrogen atoms from four different DIB ligands and two fluorine atoms from two TiF_6^{2-} groups (Figs. 1(a) and 1(b)). The DIB ligand is in anti-configuration while TiF_6^{2-} is coordinating through trans mode. Six copper ions and six DIB linkers generate a very twisted loop. Every unit cell contains two adjacent narrow one-dimensional (1D) channel with fluorine atoms decorated in the surface (Fig. 1(c)). The solvents play an important role in the self-assembly of the building units. In MeOH/H_2O solution, needle-shaped purple crystals of ZNU-5 were cultivated with distinct porous structures (Fig. S2(b) in the ESM). As shown in Fig. 1(d), every Cu(II) cation is octahedrally coordinated to four DIB ligands in half syn and half anti configuration and two TIFSIX anions in cis coordination mode, extending to a non-interpenetrated pcu topology framework (Fig. 1(e)). Different from ZNU-4, ZNU-5 features two-dimensional pore channels as shown in Fig. 1(f).

As shown in Fig. 2(a), the powder X-ray diffraction (PXRD) patterns of the as-synthesized ZNU-5 are consistent with the simulated ones from crystal structure, indicating the pure phase of sample. ZNU-5 is relatively stable in humid air but sensitive to water. A new phase appears when the sample is immersed in water. Interestingly, the original phase can be recovered when the water-soaked samples were re-activated or re-soaked in methanol (Fig. S12 in the ESM). Thermo gravimetric analysis (TGA) analysis was conducted to compare the thermal stability of ZNU-4 and ZNU-5 qualitatively (Fig. 2(b)). The weight reduction before 150 °C belongs to the loss of water and organic solvent in the pores. ZNU-5 shows a second weight loss until 340 °C, slightly higher than that of ZNU-4 (290 °C), suggesting the superior thermal stability of ZNU-5.

3.2 Single-component adsorption experiments and selectivity calculations

To evaluate the pore properties of ZNU-4 and ZNU-5, CO_2 adsorption measurements were performed at 195 K (Fig. 3(a)). ZNU-4 displays the type-I isotherm and the maximum loading is 105.7 cm^3/g at 100 kPa. The Brunauer–Emmett–Teller (BET) surface area is 358.6 m^2/g. In contrast, two stages of CO_2 adsorption are observed for ZNU-5. The CO_2 uptakes in the first and second steps are 200.9 (15 kPa) and 299.8 cm^3/g (100 kPa), respectively. The BET surface area is 751.5 m^2/g (Fig. S14(b) in the ESM). The calculated pore width is 5.2 Å (Fig. S14(a) in the ESM), perfectly consistent with the pore size (5.2 Å) measured from the single crystal structure (Fig. S10 in the ESM).

The distinct structure/pore architectures and porosity of ZNU-4 and ZNU-5 prompted us to evaluate their difference in gas

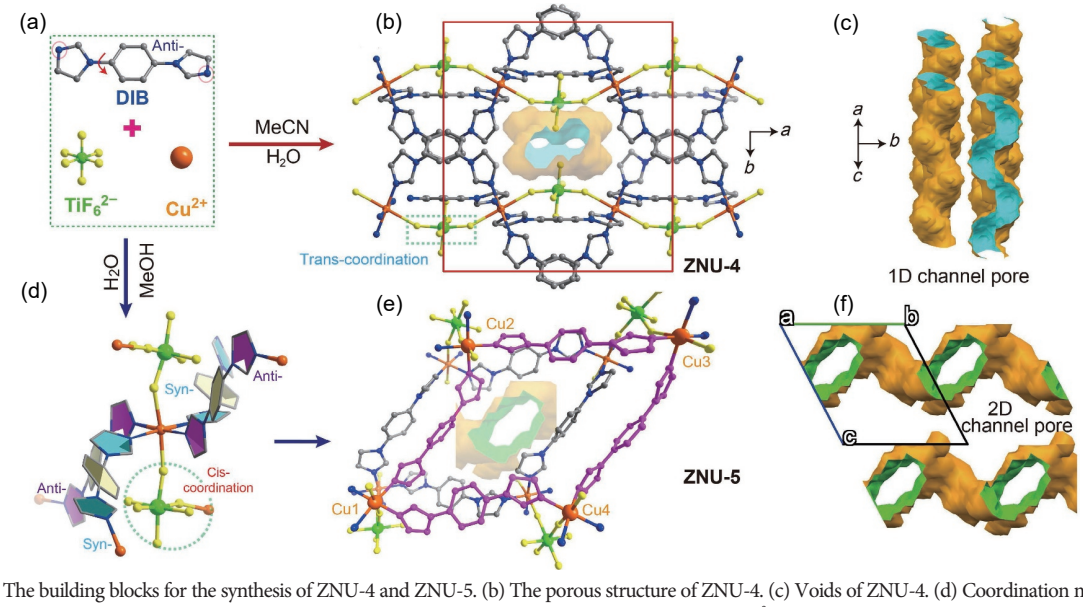

Figure 1 (a) The building blocks for the synthesis of ZNU-4 and ZNU-5. (b) The porous structure of ZNU-4. (c) Voids of ZNU-4. (d) Coordination mode in ZNU-5. (e) The porous structure of ZNU-5. (f) Voids of ZNU-5. The voids are generated by a probe with a radius of 1.2 Å.

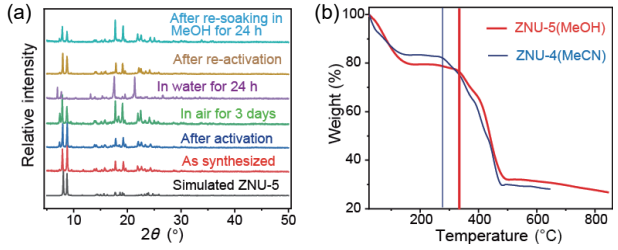

Figure 2 (a) PXRD patterns of ZNU-5 under different condition. (b) Thermo gravimetric analysis curve of ZNU-4 and ZNU-5.

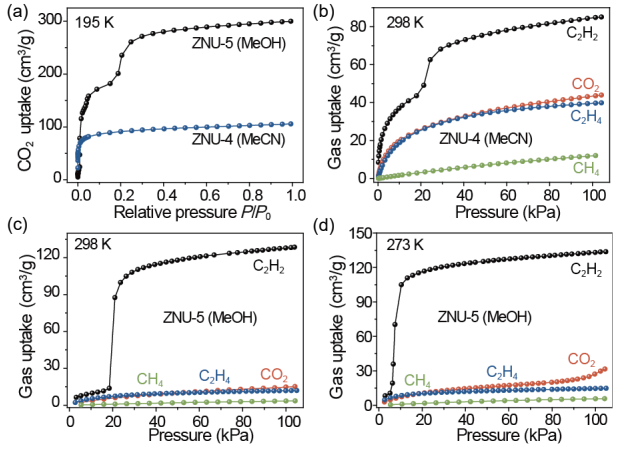

Figure 3 (a) CO_2 adsorption isotherm for ZNU-4 and ZNU-5 at 195 K. (b) C_2H_2, CO_2, C_2H_4, and CH_4 adsorption isotherms in ZNU-4 at 298 K. (c) and (d) C_2H_2, CO_2, C_2H_4, and CH_4 adsorption isotherms in ZNU-5 at 298 and 273 K.

adsorption and separation performances. As shown in Figs. 3(b)–3(d), and Figs. S15 and S16 in the ESM, we performed unary gas adsorption tests for C_2H_2, CO_2, C_2H_4, and CH_4 under the temperature ranging from 263 to 313 K. The C_2H_2 adsorption isotherms of ZNU-5 showed gate-opening pressure increases from 5 kPa (273 K) to around 20 kPa (298 K) and 30 kPa (313 K), indicating that the gate-opening pressure is temperature dependent. Such temperature dependent gate-opening has also been observed for CO_2 at 263 K, which possesses a higher gate-opening pressure (65 kPa). Impressively, ZNU-5 exhibits a remarkably high C_2H_2 uptake of 128.6 cm^3/g at 298 K and 100 kPa with a flexible feature (Fig. 3(c)), which is 51.1% higher than that of ZNU-4 (85.1 cm^3/g). This value sets a new record of C_2H_2 capacity at 100 kPa among MOF materials with C_2H_2/CO_2 molecular sieving effect, which outperforms many benchmark MOFs including UTSA-300 (69.0 cm^3/g) [31], NTU-65 (75.4 cm^3/g) [35], ZJU-196 (83.5 cm^3/g) [36], CPL-1-NH_2 (41.2 cm^3/g) [37], SIFSIX-dps-Cu (102.4 cm^3/g) [32], and MOF-OH (60.0 cm^3/g) [38]. Notably, ZNU-5 completely prevents the CO_2, C_2H_4, and CH_4 entrance at the pressure up to 100 kPa at 298 K. Therefore, the exceptional C_2H_2 capture capacity at 100 kPa combined with the much lower CO_2, C_2H_4, and CH_4 uptakes enables ZNU-5 with great potential to achieve one-step C_2H_2 purification from quaternary $C_2H_2/CO_2/C_2H_4/CH_4$ mixtures.

Figure 4(a) shows that the initial Q_{st} values for C_2H_2 (27.8 kJ/mol) in ZNU-5 is much lower than that of ZNU-4 (50.3 kJ/mol), implying a relatively low energy consumption in regeneration.

IAST calculations were performed to qualitatively evaluate the adsorption selectivity of ZNU-4 and ZNU-5 for equimolar C_2H_2/CO_2, C_2H_2/C_2H_4, and C_2H_2/CH_4 mixtures at 298 K, respectively. Due to the existence of the gate-opening phenomenon, the fitting is challenging and temperature dependant dual-site Langmuir–Freundlich model is applied. The comparison of experimental and simulated adsorption isotherms

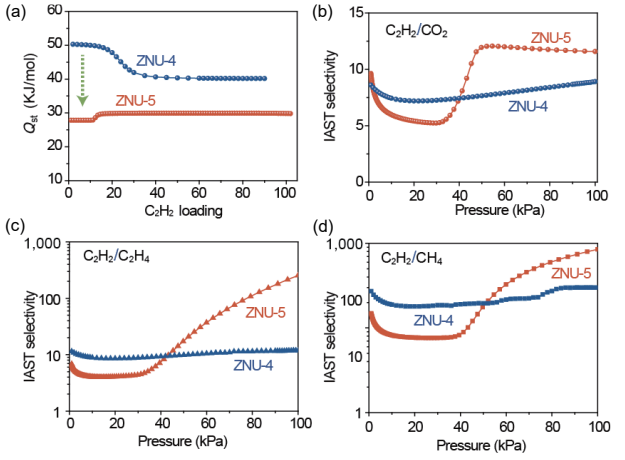

Figure 4 (a) Q_{st} for C_2H_2 adsorption in ZNU-4 and ZNU-5. (b)–(d) IAST selectivity for equimolar C_2H_2/CO_2, C_2H_2/C_2H_4, and C_2H_2/CH_4 mixtures in ZNU-4 and ZNU-5 at 298 K.

as well as the fitting parameters are presented in Fig. S17 and Table S3 in the ESM, which showed the fitting is in excellent accuracy. For equimolar C_2H_2/CO_2, C_2H_2/C_2H_4, and C_2H_2/CH_4 mixtures, as presented in Figs. 4(b)–4(d), ZNU-5 exhibits a higher selectivity up to 12, 255, and 850 at 100 kPa, which is superior to ZNU-4 with the selectivity of 9, 12, and 300.

The comparison of C_2H_2 and CO_2 uptake in top-performing materials is presented in Fig. 5(a). ZNU-5 is the best example that shows a very high C_2H_2 uptake as well as a very low CO_2 uptake, which is also reflected in the C_2H_2/CO_2 uptake ratio in Fig. 5(b). SNNU-65-Cu-Sc [39], MIL-160 [40], FJU-90 [41], SIFSIX-Cu-TPA [42], and SIFSIX-1-Cu [43] exhibited a higher C_2H_2 uptake, yet a higher CO_2 uptake as well, leading to decreased C_2H_2/CO_2 selectivity. Besides, ZNU-5 is the only porous materials that exhibit a C_2H_2/CO_2 uptake ratio > 8 and Q_{st} value < 30 kJ/mol [44–53]. A more comprehensive comparison table is listed in Tables S4–S6 in the ESM, among which ZNU-5 is still a benchmark material for C_2H_2 recovery from other gases.

3.3 Dynamic breakthrough experiments

Transient breakthrough simulations were conducted to evaluate the separation performance of ZNU-5 for equimolar C_2H_2/CO_2 (50/50) mixture. As shown in Fig. 6, ZNU-5 exhibits a stepped breakthrough curve for C_2H_2, which is not seen in rigid adsorbents [54]. Nonetheless, the captured C_2H_2 amount is still very large while that of CO_2 is negligible, thus leading to a high separation factor. Besides, as C_2H_2, the target gas, needs desorption process to obtain, slight leakage in the breakthrough process will not have large influence on the dynamic capacity of C_2H_2.

To evaluate the practical separation performance as well as confirm the stepped breakthrough phenomenon, experimental breakthrough tests were conducted. The results showed that the experimental breakthrough curves are very similar with the simulations (Fig. S18 in the ESM). For equimolar C_2H_2/CO_2 mixtures, efficient separations could be accomplished by ZNU-5

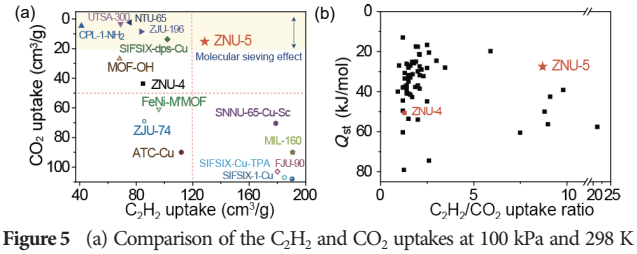

Figure 5 (a) Comparison of the C_2H_2 and CO_2 uptakes at 100 kPa and 298 K between ZNU-5 and other materials. (b) Comparison of C_2H_2/CO_2 uptake ratio and Q_{st} for C_2H_2 between ZNU-5 and other materials.

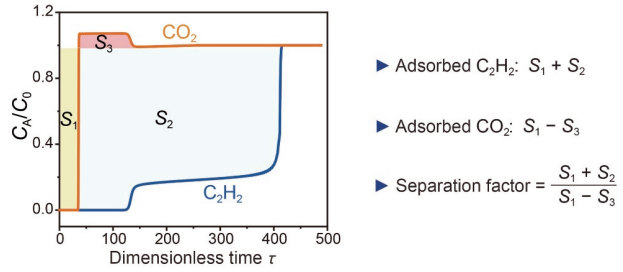

Figure 6 Simulated breakthrough curve of ZNU-5 for C_2H_2/CO_2 (50/50) at 298 K.

with 3.3 mol/g of C_2H_2 capacity, while the uptake of C_2H_2 absorbed in ZNU-4 was only 2.2 mol/g (Fig. 7(a)). Subsequently, we explored the effect of different desorption temperatures on regeneration. Figure 7(b) shows that the desorption time of C_2H_2 is gradually shortened with the increase of desorption temperature. Controlling the desorption temperature of 25 °C, 2.6 mol/g of 98% purity C_2H_2 can be recovered from the column after blowing CO_2 out at the first stage. The dynamic separation factor of C_2H_2/CO_2 is calculated to be 9.1 (Fig. S20 in the ESM), higher than those of ZNU-4 (5.4) [34] and many other top-performing materials such as CAU-10-H (3.4) [53] , JCM-1 (4.4) [45], ZJU-74a (4.3) [55], and SNNU-45 (2.9) [8]. The capture ability of ZNU-5 for C_2H_2 from the ternary and quaternary mixtures was further studied. As shown in Figs. 7(c) and 7(d), when the gas mixtures containing equal ratios of $C_2H_2/CO_2/CH_4$ or $C_2H_2/CO_2/CH_4/C_2H_4$ passed through the ZNU-5 packed column, CO_2/CH_4 or $CO_2/CH_4/C_2H_4$ outflowed first, then C_2H_2 began to discharge at around 104/170 min, and up to 2.8/2.2 mmol/g of C_2H_2 was adsorbed in this process. During desorption process, 2.0/1.5 mmol/g of 98% purity C_2H_2 can be recovered from the column by stepped Ar purge process, which are both higher than those of ZNU-4 (0.48 and 0.05 mmol/g) [34].

Recycability is a very important parameter to assess the potential for practical application. Thus, 5 repetitive breakthrough experiments were carried out. Negligible capacity reduction is observed (Fig. 8), demonstrating that ZNU-5 is a promising adsorbent with good cyclic utilization performance.

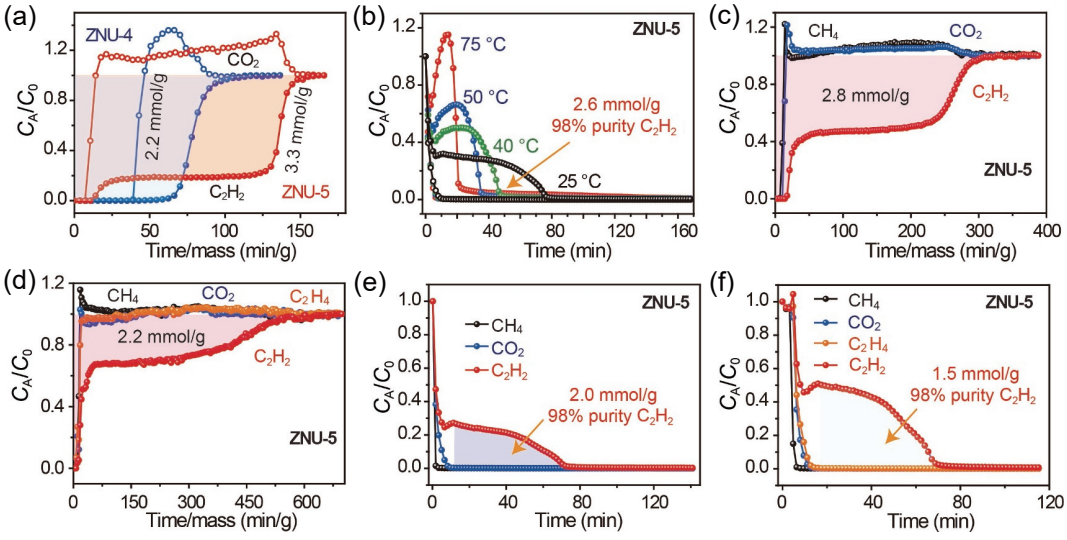

Figure 7 (a) The breakthrough curve for C_2H_2/CO_2 (50/50) separation at ZNU-4 and ZNU-5. (b) The C_2H_2/CO_2 (50/50) desorption curves for ZNU-5 at 25, 40, 50, and 75 °C. (c) The breakthrough curve for $C_2H_2/CO_2/CH_4$ (33.3/33.3/33.3) separation at ZNU-5. (d) The breakthrough curves for $C_2H_2/CO_2/C_2H_4/CH_4$ (25/25/25/25) separation at ZNU-5. (e) The desorption curves for $C_2H_2/CO_2/CH_4$ (33.3/33.3/33.3) separation at ZNU-5. (f) The desorption curves for $C_2H_2/CO_2/C_2H_4/CH_4$ (25/25/25/25) separation at ZNU-5.

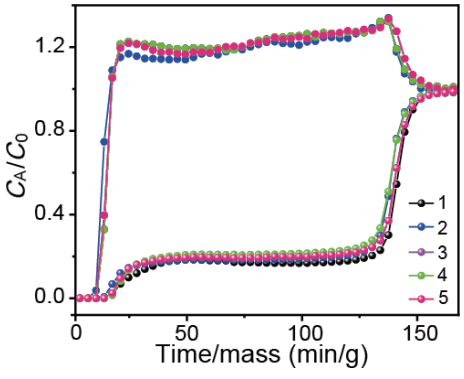

Figure 8 Five cycles of dynamic breakthrough curves for C_2H_2/CO_2 (50/50, v/v) mixture.

4 Conclusions

In a nutshell, we reported a novel fluorinated anion pillared MOF with flexible molecular sieving effect that can efficiently capture C_2H_2 from CO_2 and C_nH_4 (n = 1 and 2). The foregoing results revealed that ZNU-5 exhibits not only high C_2H_2 uptake capacity but also simultaneously excellent C_2H_2/CO_2 (12), C_2H_2/C_2H_4 (255), and C_2H_2/CH_4 (850) selectivity under ambient conditions, outperforming most of the flexible molecular sieving MOFs reported. Experimental breakthrough tests further confirmed the effective capture of C_2H_2 from binary C_2H_2/CO_2, ternary $C_2H_2/CO_2/CH_4$, and quaternary $C_2H_2/CO_2/CH_4/C_2H_4$ mixtures with large productivity and good recycability. Thus, combining large working capacity, low adsorption heat, as well as excellent recyclability, ZNU-5 is a promising adsorbent for practical C_2H_2 purification and separation. The mechanism of the selective gate opening behavior is under study.

Acknowledgements

Y. B. Z. acknowledged the financial support by the National Natural Science Foundation of China (No. 21908193) and Jinhua Industrial Key Project (No. 2021A22648). S. D. acknowledged the financial support by the National Natural Science Foundation of China (No. 21871231) and the Special Funds for Basic Scientific Research of Zhejiang University (Nos. 2019QNA3010 and K20210335). L. Y. W. acknowledged the financial support by the

National Natural Science Foundation of China (No. 22205207).

Electronic Supplementary Material: Supplementary material (crystallographic data and additional figures) is available in the online version of this article at https://doi.org/10.1007/s12274-022-4996-9.

References

[1] Weissermel, K.; Arpe, H. J. *Industrial Organic Chemistry*, 4th ed.; Wiley-VCH: Weinheim, 2003.

[2] Zhang, Y. B.; Hu, J. B.; Krishna, R.; Wang, L. Y.; Yang, L. F.; Cui, X. L.; Duttwyler, S.; Xing, H. B. Rational design of microporous MOFs with anionic boron cluster functionality and cooperative dihydrogen binding sites for highly selective capture of acetylene. *Angew. Chem., Int. Ed.* **2020**, *59*, 17664–17669.

[3] Moreau, F.; da Silva, I.; Al Smail, N. H.; Easun, T. L.; Savage, M.; Godfrey, H. G. W.; Parker, S. F.; Manuel, P.; Yang, S. H.; Schröder, M. Unravelling exceptional acetylene and carbon dioxide adsorption within a tetra-amide functionalized metal-organic framework. *Nat. Commun.* **2017**, *8*, 14085.

[4] Fan, W. D.; Wang, X.; Liu, X. P.; Xu, B.; Zhang, X. R.; Wang, W. J.; Wang, X. K.; Wang, Y. T.; Dai, F. N.; Yuan, D. Q. et al. Regulating C_2H_2 and CO_2 storage and separation through pore environment modification in a microporous Ni-MOF. *ACS Sustainable Chem. Eng.* **2019**, *7*, 2134–2140.

[5] Wang, G. D.; Wang, H. H.; Shi, W. J.; Hou, L.; Wang, Y. Y.; Zhu, Z. H. A highly stable MOF with F and N accessible sites for efficient capture and separation of acetylene from ternary mixtures. *J. Mater. Chem. A* **2021**, *9*, 24495–24502.

[6] Foo, M. L.; Matsuda, R.; Hijikata, Y.; Krishna, R.; Sato, H.; Horike, S.; Hori, A.; Duan, J. G.; Sato, Y.; Kubota, Y. et al. An adsorbate discriminatory gate effect in a flexible porous coordination polymer for selective adsorption of CO_2 over C_2H_2. *J. Am. Chem. Soc.* **2016**, *138*, 3022–3030.

[7] Wang, Q. J.; Hu, J. B.; Yang, L. F.; Zhang, Z. Q.; Ke, T.; Cui, X. L.; Xing, H. B. One-step removal of alkynes and propadiene from cracking gases using a multi-functional molecular separator. *Nat. Commun.* **2022**, *13*, 2955.

[8] Li, Y. P.; Wang, Y.; Xue, Y. Y.; Li, H. P.; Zhai, Q. G.; Li, S. N.; Jiang, Y. C.; Hu, M. C.; Bu, X. H. Ultramicroporous building units as a path to Bi-microporous metal-organic frameworks with high acetylene storage and separation performance. *Angew. Chem., Int. Ed.* **2019**, *58*, 13590–13595.

[9] Niu, Z.; Cui, X. L.; Pham, T.; Verma, G.; Lan, P. C.; Shan, C.; Xing, H. B.; Forrest, K. A.; Suepaul, S.; Space, B. et al. A MOF-based ultra-strong acetylene nano-trap for highly efficient C_2H_2/CO_2 separation. *Angew. Chem., Int. Ed.* **2021**, *60*, 5283–5288.

[10] Zhang, L.; Jiang, K.; Yang, L. F.; Li, L. B.; Hu, E. L.; Yang, L.; Shao, K.; Xing, H. B.; Cui, Y. J.; Yang, Y. et al. Benchmark C_2H_2/CO_2 separation in an ultra-microporous metal-organic framework via copper(I)-alkynyl chemistry. *Angew. Chem., Int. Ed.* **2021**, *60*, 15995–16002.

[11] Sun, W. Q.; Hu, J. B.; Jiang, Y. J.; Xu, N.; Wang, L. Y.; Li, J. H.; Hu, Y. Q.; Duttwyler, S.; Zhang, Y. B. Flexible molecular sieving of C_2H_2 from CO_2 by a new cost-effective metal organic framework with intrinsic hydrogen bonds. *Chem. Eng. J.* **2022**, *439*, 135745.

[12] Di, Z. Y.; Pang, J. D.; Hu, F. L.; Wu, M. Y.; Hong, M. C. An ultra-stable microporous supramolecular framework with highly selective adsorption and separation of water over ethanol. *Nano Res.* **2021**, *14*, 2584–2588.

[13] Fan, W. D.; Yuan, S.; Wang, W. J.; Feng, L.; Liu, X. P.; Zhang, X. R.; Wang, X.; Kang, Z. X.; Dai, F. N.; Yuan, D. Q. et al. Optimizing multivariate metal-organic frameworks for efficient C_2H_2/CO_2 separation. *J. Am. Chem. Soc.* **2020**, *142*, 8728–8737.

[14] Liu, Y.; Xu, Q. Q.; Chen, L. H.; Song, C. H.; Yang, Q. W.; Zhang, Z. G.; Lu, D.; Yang, Y. W.; Ren, Q. L.; Bao, Z. B. Hydrogen-bonded metal-nucleobase frameworks for highly selective capture of ethane/propane from methane and methane/nitrogen separation. *Nano Res.* **2022**, *15*, 7695–7702.

[15] Chen, S.; Behera, N.; Yang, C.; Dong, Q. B.; Zheng, B. S.; Li, Y. Y.; Tang, Q.; Wang, Z. X.; Wang, Y. Q.; Duan, J. G. A chemically stable nanoporous coordination polymer with fixed and free Cu^{2+} ions for boosted C_2H_2/CO_2 separation. *Nano Res.* **2021**, *14*, 546–553.

[16] Cui, J. Y.; Zhang, Z. Q.; Tan, B.; Zhang, Y. B.; Wang, P. C.; Cui, X. L.; Xing, H. B. Efficient separation of n-butene and iso-butene by flexible ultramicroporous metal-organic frameworks with pocket-like cavities. *Chem.—Asian J.* **2019**, *14*, 3572–3576.

[17] Fu, X. P.; Wang, Y. L.; Zhang, X. F.; Krishna, R.; He, C. T.; Liu, Q. Y.; Chen, B. L. Collaborative pore partition and pore surface fluorination within a metal-organic framework for high-performance C_2H_2/CO_2 separation. *Chem. Eng. J.* **2022**, *432*, 134433.

[18] Duan, J. G.; Higuchi, M.; Zheng, J. J.; Noro, S. I.; Chang, I. Y.; Hyeon-Deuk, K.; Mathew, S.; Kusaka, S.; Sivaniah, E.; Matsuda, R. et al. Density gradation of open metal sites in the mesospace of porous coordination polymers. *J. Am. Chem. Soc.* **2017**, *139*, 11576–11583.

[19] Sharma, S.; Mukherjee, S.; Desai, A. V.; Vandichel, M.; Dam, G. K.; Jadhav, A.; Kociok-Köhn, G.; Zaworotko, M. J.; Ghosh, S. K. Efficient capture of trace acetylene by an ultramicroporous metal-organic framework with purine binding sites. *Chem. Mater.* **2021**, *33*, 5800–5808.

[20] Sun, W. Q.; Hu, J. B.; Duttwyler, S.; Wang, L. Y.; Krishna, R.; Zhang, Y. B. Highly selective gas separation by two isostructural boron cluster pillared MOFs. *Sep. Purif. Technol.* **2022**, *283*, 120220.

[21] Wang, G. D.; Li, Y. Z.; Zhang, W. F; Hou, L.; Wang, Y. Y.; Zhu, Z. H. Acetylene separation by a Ca-MOF containing accessible sites of open metal centers and organic groups. *ACS Appl. Mater. Interfaces* **2021**, *13*, 58862–58870.

[22] Yang, L. F.; Qian, S. H.; Wang, X. B.; Cui, X. L.; Chen, B. L.; Xing, H. B. Energy-efficient separation alternatives: Metal-organic frameworks and membranes for hydrocarbon separation. *Chem. Soc. Rev.* **2020**, *49*, 5359–5406.

[23] Zhang, Y. B.; Cui, X. L.; Xing, H. B. Recent advances in the capture and abatement of toxic gases and vapors by metal-organic frameworks. *Mater. Chem. Front.* **2021**, *5*, 5970–6013.

[24] Zhang, Z.; Peh, S. B.; Wang, Y. X.; Kang, C. J.; Fan, W. D.; Zhao, D. Efficient trapping of trace acetylene from ethylene in an ultramicroporous metal-organic framework: Synergistic effect of high-density open metal and electronegative sites. *Angew. Chem., Int. Ed.* **2020**, *59*, 18927–18932.

[25] Fan, W. D.; Wang, X.; Zhang, X. R.; Liu, X. P.; Wang, Y. T.; Kang, Z. X.; Dai, F. N.; Xu, B.; Wang, R. M.; Sun, D. F. Fine-tuning the pore environment of the microporous Cu-MOF for high propylene storage and efficient separation of light hydrocarbons. *ACS Cent. Sci.* **2019**, *5*, 1261–1268.

[26] Zeng, H.; Xie, M.; Huang, Y. L.; Zhao, Y. F.; Xie, X. J.; Bai, J. P.; Wan, M. Y.; Krishna, R.; Lu, W. G.; Li, D. Induced fit of C_2H_2 in a flexible MOF through cooperative action of open metal sites. *Angew. Chem., Int. Ed.* **2019**, *58*, 8515–8519.

[27] Fan, W. D.; Ying, Y. P.; Peh, S. B.; Yuan, H. Y.; Yang, Z. Q.;Yuan, Y. D.; Shi, D. C.; Yu, X.; Kang, C. J.; Zhao, D. Multivariate polycrystalline metal-organic framework membranes for CO_2/CH_4 separation. *J. Am. Chem. Soc.* **2021**, *143*, 17716–17723.

[28] Jiang, Y. J.; Hu, J. B.; Wang, L. Y.; Sun, W. Q.; Xu, N.; Krishna, R.; Duttwyler, S.; Cui, X. L.; Xing, H. B.; Zhang, Y. B. Comprehensive pore tuning in an ultrastable fluorinated anion cross-linked cage-like MOF for simultaneous benchmark propyne recovery and propylene purification. *Angew. Chem., Int. Ed.* **2022**, *61*, e202200947.

[29] Li, S. L.; Zeng, S. L.; Tian, Y. Y.; Jing, X. F.; Sun, F. X.; Zhu, G. S. Two flexible cationic metal-organic frameworks with remarkable stability for CO_2/CH_4 separation. *Nano Res.* **2021**, *14*, 3288–3293.

[30] Wang, L. Y.; Jiang, T.; Duttwyler, S.; Zhang, Y. B. Supramolecular Cu(II)-dipyridyl frameworks featuring weakly coordinating dodecaborate dianions for selective gas separation. *CrystEngComm* **2021**, *23*, 282–291.

[31] Lin, R. B.; Li, L. B.; Wu, H.; Arman, H.; Li, B.; Lin, R. G.; Zhou, W.; Chen, B. L. Optimized separation of acetylene from carbon dioxide and ethylene in a microporous material. *J. Am. Chem. Soc.*

2017, *139*, 8022–8028.
[32] Wang, J.; Zhang, Y.; Su, Y.; Liu, X.; Zhang, P. X.; Lin, R. B.; Chen, S. X.; Deng, Q.; Zeng, Z. L.; Deng, S. G. et al. Fine pore engineering in a series of isoreticular metal-organic frameworks for efficient C_2H_2/CO_2 separation. *Nat. Commun.* **2022**, *13*, 200.
[33] Wang, L. Y.; Sun, W. Q.; Zhang, Y. B.; Xu, N.; Krishna, R.; Hu, J. B.; Jiang, Y. J.; He, Y. B.; Xing, H. B. Interpenetration symmetry control within ultramicroporous robust boron cluster hybrid MOFs for benchmark purification of acetylene from carbon dioxide. *Angew. Chem., Int. Ed.* **2021**, *60*, 22865–22870.
[34] Xu, N.; Hu, J. B.; Wang, L. Y.; Luo, D.; Sun, W. Q.; Hu, Y. Q.; Wang, D. M.; Cui, X. L.; Xing, H. B.; Zhang, Y. B. A TIFSIX pillared MOF with unprecedented zsd topology for efficient separation of acetylene from quaternary mixtures. *Chem. Eng. J.* **2022**, *450*, 138034.
[35] Dong, Q. B.; Zhang, X.; Liu, S.; Lin, R. B.; Guo, Y. N.; Ma, Y. S.; Yonezu, A.; Krishna, R.; Liu, G. P.; Duan, J. G. et al. Tuning gate-opening of a flexible metal-organic framework for ternary gas sieving separation. *Angew. Chem., Int. Ed.* **2020**, *59*, 22756–22762.
[36] Zhang, L.; Jiang, K.; Li, L. B.; Xia, Y. P.; Hu, T. L.; Yang, Y.; Cui, Y. J.; Li, B.; Chen, B. L.; Qian, G. D. Efficient separation of C_2H_2 from C_2H_2/CO_2 mixtures in an acid-base resistant metal-organic framework. *Chem. Commun.* **2018**, *54*, 4846–4849.
[37] Yang, L. Z.; Yan, L. T.; Wang, Y.; Liu, Z.; He, J. X.; Fu, Q. J.; Liu, D. D.; Gu, X.; Dai, P. C.; Li, L. J.; Zhao, X. B. Adsorption site selective occupation strategy within a metal-organic framework for highly efficient sieving acetylene from carbon dioxide. *Angew. Chem., Int. Ed.* **2021**, *60*, 4570–4574.
[38] Gong, W.; Cui, H.; Xie, Y.; Li, Y. G.; Tang, X. H.; Liu, Y.; Cui, Y.; Chen, B. L. Efficient C_2H_2/CO_2 separation in ultramicroporous metal-organic frameworks with record C_2H_2 storage density. *J. Am. Chem. Soc.* **2021**, *143*, 14869–14876.
[39] Zhang, J. W.; Hu, M. C.; Li, S. N.; Jiang, Y. C.; Qu, P.; Zhai, Q. G. Assembly of $[Cu_2(COO)_4]$ and $[M_3(\mu_3\text{-}O)(COO)_6]$ (M = Sc, Fe, Ga, and In) building blocks into porous frameworks towards ultra-high C_2H_2/CO_2 and C_2H_2/CH_4 separation performance. *Chem. Commun.* **2018**, *54*, 2012–2015.
[40] Ye, Y. X.; Xian, S. K.; Cui, H.; Tan, K.; Gong, L. S.; Liang, B.; Pham, T.; Pandey, H.; Krishna, R.; Lan, P. C. et al. Metal-organic framework based hydrogen-bonding nanotrap for efficient acetylene storage and separation. *J. Am. Chem. Soc.* **2022**, *144*, 1681–1689.
[41] Ye, Y. X.; Ma, Z. L.; Lin, R. B.; Krishna, R.; Zhou, W; Lin, Q. J.; Zhang, Z. J.; Xiang, S. C.; Chen, B. L. Pore space partition within a metal-organic framework for highly efficient C_2H_2/CO_2 separation. *J. Am. Chem. Soc.* **2019**, *141*, 4130–4136.
[42] Li, H.; Liu, C. P.; Chen, C.; Di, Z. Y.; Yuan, D. Q.; Pang, J. D.; Wei, W.; Wu, M. Y.; Hong, M. C. An unprecedented pillar-cage fluorinated hybrid porous framework with highly efficient acetylene storage and separation. *Angew. Chem., Int. Ed.* **2021**, *60*, 7547–7552.
[43] Cui, X. L.; Chen, K. J.; Xing, H. B.; Yang, Q. W.; Krishna, R.; Bao, Z. B.; Wu, H.; Zhou, W.; Dong, X. L.; Han, Y. et al. Pore chemistry and size control in hybrid porous materials for acetylene capture from ethylene. *Science.* **2016**, *353*, 141–144.
[44] Dutta, S.; Mukherjee, S.; Qazvini, O. T.; Gupta, A. K.; Sharma, S.; Mahato, D.; Babarao, R.; Ghosh, S. K. Three-in-one C_2H_2-selectivity-guided adsorptive separation across an isoreticular family of cationic square-lattice MOFs. *Angew. Chem., Int. Ed.* **2022**, *61*, e202114132.
[45] Lee, J.; Chuah, C. Y.; Kim, J.; Kim, Y.; Ko, N.; Seo, Y.; Kim, K.; Bae, T. H.; Lee, E. Separation of acetylene from carbon dioxide and ethylene by a water-stable microporous metal-organic framework with aligned imidazolium groups inside the channels. *Angew. Chem., Int. Ed.* **2018**, *57*, 7869–7873.
[46] Mukherjee, S.; He, Y. H.; Franz, D.; Wang, S. Q.; Xian, W. R.; Bezrukov, A. A.; Space, B.; Xu, Z. T.; He, J.; Zaworotko, M. J. Halogen-C_2H_2 binding in ultramicroporous metal-organic frameworks (MOFs) for benchmark C_2H_2/CO_2 separation selectivity. *Chem.—Eur. J.* **2020**, *26*, 4923–4929.
[47] Zhao, J. Y.; Li, Q.; Zhu, X. C.; Li, J.; Wu, D. P. Highly robust tetranuclear cobalt-based 3D framework for efficient C_2H_2/CO_2 and C_2H_2/C_2H_4 separations. *Inorg. Chem.* **2020**, *59*, 14424–14431.
[48] Meng, L. K.; Yang, L. X.; Chen, C. L.; Dong, X. L.; Ren, S. Y.; Li, G. H.; Li, Y.; Han, Y.; Shi, Z.; Feng, S. H. Selective acetylene adsorption within an imino-functionalized nanocage-based metal-organic framework. *ACS Appl. Mater. Interfaces* **2020**, *12*, 5999–6006.
[49] Peng, Y. L.; Pham, T.; Li, P. F.; Wang, T.; Chen, Y.; Chen, K. J.; Forrest, K. A.; Space, B.; Cheng, P.; Zaworotko, M. J. et al. Robust ultramicroporous metal-organic frameworks with benchmark affinity for acetylene. *Angew. Chem., Int. Ed.* **2018**, *57*, 10971–10975.
[50] Zhang, J. P.; Chen, X. M. Optimized acetylene/carbon dioxide sorption in a dynamic porous crystal. *J. Am. Chem. Soc.* **2009**, *131*, 5516–5521.
[51] Zhang, X.; Lin, R. B.; Wu, H.; Huang, Y. H.; Ye, Y. X.; Duan, J. G.; Zhou, W.; Li, J. R.; Chen. B. L. Maximizing acetylene packing density for highly efficient C_2H_2/CO_2 separation through immobilization of amine sites within a prototype MOF. *Chem. Eng. J.* **2022**, *431*, 134184.
[52] Zhang, Y. B.; Wang, L. Y.; Hu, J. B.; Duttwyler, S.; Cui, X. L.; Xing, H. B. Solvent-dependent supramolecular self-assembly of boron cage pillared metal-organic frameworks for selective gas separation. *CrystEngComm* **2020**, *22*, 2649–2655.
[53] Pei, J. Y.; Wen, H. M.; Gu, X. W.; Qian, Q. L.; Yang, Y.; Cui, Y. J.; Li, B.; Chen, B. L.; Qian, G. D. Dense packing of acetylene in a stable and low-cost metal-organic framework for efficient C_2H_2/CO_2 separation. *Angew. Chem., Int. Ed.* **2021**, *60*, 25068–25074.
[54] Sotomayor, F. J.; Lastoskie, C. M. Predicting the breakthrough performance of "gating" adsorbents using osmotic framework-adsorbed solution theory. *Langmuir* **2017**, *33*, 11670–11678.
[55] Pei, J. Y.; Shao, K.; Wang, J. X.; Wen, H. M.; Yang, Y.; Cui, Y. J.; Krishna, R.; Li, B.; Qian, G. D. A chemically stable hofmann-type metal-organic framework with sandwich-like binding sites for benchmark acetylene capture. *Adv. Mater.* **2020**, *32*, 1908275.

Electronic Supplementary Material

Efficient capture of C_2H_2 from CO_2 and C_nH_4 by a novel fluorinated anion pillared MOF with flexible molecular sieving effect

Lingyao Wang[1], Nuo Xu[1], Yongqi Hu[1], Wanqi Sun[1], Rajamani Krishna[2], Jiahao Li[1], Yunjia Jiang[1], Simon Duttwyler[3], and

Yuanbin Zhang[1] (✉)

[1] *Key Laboratory of the Ministry of Education for Advanced Catalysis Materials, College of Chemistry and Life Sciences, Zhejiang Normal University, Jinhua 321004, China*
[2] *Van't Hoff Institute for Molecular Sciences, University of Amsterdam, Science Park 904, Amsterdam 1098 XH, the Netherlands*
[3] *Department of Chemistry, Zhejiang University, Hangzhou 310027, China*

Supporting information to https://doi.org/10.1007/s12274-022-4996-9

Address correspondence to ybzhang@zjnu.edu.cn

Experimental Section

I. General Information and Procedures

Materials:

1,4-dibromobenzene, CuI, and dimethylglycine were purchased from Energy Chemical. $Cu(NO_3)_2{\cdot}3H_2O$ was purchased from Macklin. $(NH_4)_2TiF_6$ was purchased from Alab Chemical Technology. Imidazole was purchased from Aladdin. K_2CO_3 was purchased from LUQUAN without further purification. All reagents and solvents were used without further purification.

Procedures:

1,4-di(1H-imidazol-1-yl)benzene was synthesized according to the literature method with slight modifications[1] :A mixture of 1,4-dibromobenzene (4.718 g, 20 mmol), imidazole (3.404 g, 50 mmol), K_2CO_3 (11.057 g, 80 mmol), dimethylglycine (825.0 mg, 8 mmol) and CuI (761.8 mg, 4 mmol) were charged into a Schlenk flask. The system was then evacuated and back filled with N_2 twice, followed by addition of 50 mL of DMSO. The mixture was heated at 110 °C for 48 h before it was partitioned between water and ethyl acetate. The organic layer was separated, and the aqueous layer was extracted with ethyl acetate. The combined organic layers were washed with brine, dried over Na_2SO_4, and concentrated in vacuo. During the concentration process, white crystalline solid formed and the remaining yellow liquid (~ 10 mL) was difficult to remove under 50 °C. Then, the mixture was filtered and white solid was collected and dried under vacuum at room temperature for 2h. The purity of the obtained white solid was confirmed by 1H NMR. The weight was 2.544g. Yield: 61%.

References:

[1] Zhang, S.; Yang, S.; Lan, J.; Yang, S.; You, J. Helical nonracemic tubular coordination polymer gelators from simple achiral molecules. *Chem. Commun.* **2008**, *46*, 6170–6172.

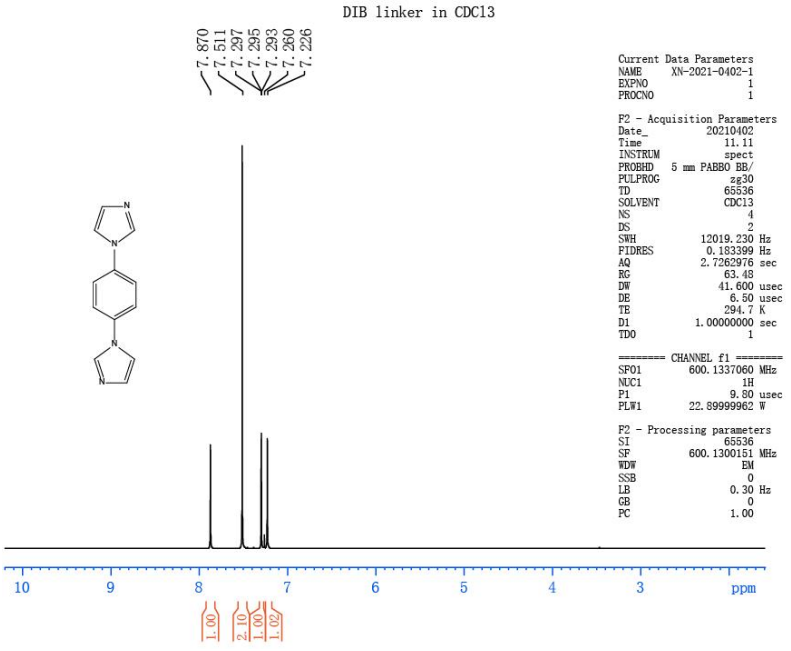

Figure S1 ^{1}H NMR spectrum of 1,4-di(1H-imidazol-1-yl)benzene

Preparation of ZNU-4: To a 5 mL long thin tube was added a 1 mL of aqueous solution with $(NH_4)_2TiF_6$ (1 mg) and $Cu(NO_3)_2{\cdot}3H_2O$ (1 mg). 2 mL of MeCN/H_2O mixture was slowly layered above the solution, followed by a 1 mL of MeCN solution of 1,4-di(1H-imidazol-1-yl)benzene(2 mg). The tube was sealed and left undisturbed at RT. After several days, blue flake shaped crystals were formed on the glass surface. The average yield is ca 75%

Preparation of ZNU-5: To a 5 mL long thin tube was added a 1 mL of aqueous solution with $(NH_4)_2TiF_6$ (1 mg) and $Cu(NO_3)_2{\cdot}3H_2O$ (1 mg). 3 mL of MeOH/H_2O mixture was slowly layered above the solution, followed by a 1 mL of MeOH solution of 1,4-di(1H-imidazol-1-yl)benzene(2 mg). The tube was sealed and left undisturbed at RT. The tube was sealed and left undisturbed at RT. After several days, purple needle-shaped crystals were formed on the glass surface. The average yield is ca 75%

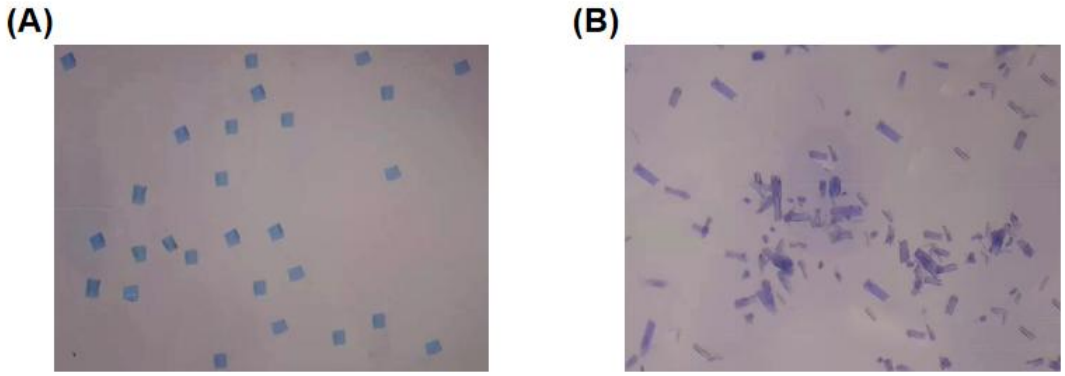

Figure S2 The microscopic image of as-synthesized ZNU-4 and ZNU-5.

Single-crystal X-ray diffraction studies were conducted at 193 K on the BrukerAXS D8 VENTURE diffractometer equipped with a PHOTON-100/CMOS detector (GaKα, λ = 1.34139 Å). Indexing was performed using APEX2. Data integration and reduction were completed using SaintPlus 6.01. Absorption correction was performed by the multi-scan method implemented in SADABS. The space group was determined using XPREP implemented in APEX2.1 The structure was solved with SHELXS-97 (direct methods) and refined on F2 (nonlinear least-squares method) with SHELXL-97 contained in APEX2, WinGX v1.70.01, and OLEX2 v1.1.5 program packages. All non-hydrogen atoms were refined anisotropically. The contribution of disordered solvent molecules was treated as diffuse using the Squeeze routine implemented in Platon.

Powder X-ray diffraction (PXRD) data were collected on the SHIMADZU XRD-6000 diffractometer (Cu Kαλ = 1.540598 Å) with an operating power of 40 KV, 30 mA and a scan speed of 4.0°/min. The range of 2θ was from 5° to 50°.

Thermal gravimetric analysis was performed on the TGA STA449F5 instrument. Experiments were carried out using a platinum pan under nitrogen atmosphere which conducted by a flow rate of 60 mL/min nitrogen gas. First, the sample was heated at 80 °C for 1 h to remove the water residue and equilibrated for 5 minutes, then cooled down to 50 °C. The data were collected at the temperature range of 50 °C to 800 °C with a ramp of 10 °C /min.

The static gas adsorption equilibrium measurements were performed on the Builder SSA 7000 (Beijing) instrument. Before gas adsorption measurements, the sample of ZNU-5 (~100 mg) was evacuated at 25 °C for 2 h firstly, and then at 80°C for 10 h until the pressure dropped below 7 μmHg. The sorption isotherms were collected at 195K, 263K, 273K, 298K, and 313K on activated samples.The

experimental temperatures were controlled by liquid acetone bath (195 K) and water / ethanol bath (263K, 273K, 298K, and 313K), respectively.

Fitting of experimental data on pure component isotherms

The unary isotherm data for C_2H_2, CO_2, CH_4, and C_2H_4 measured at four different temperatures 263K, 273K, 298K, and 313K in ZNU-5 were fitted with good accuracy using the dual-site Langmuir-Freundlich model, where we distinguish two distinct adsorption sites A and B:

$$q = \frac{q_{sat,A} b_A p^{\nu A}}{1 + b_A p^{\nu A}} + \frac{q_{sat,B} b_B p^{\nu B}}{1 + b_B p^{\nu B}} \quad \text{(S1)}$$

Here, P is the pressure of the bulk gas at equilibrium with the adsorbed phase (Pa), q is the adsorbed amount per mass of adsorbent (mol kg^{-1}), qsat, A and qsat, B are the saturation capacities of site A and B (mol kg^{-1}), b_A and b_B are the affinity coefficients of site A and B (Pa^{-1}).

In eq (S1), the Langmuir-Freundlich parameters b_A and b_B can be temperature dependent or temperature independent .

$$b_A = b_{A0} \exp\left(\frac{E_A}{RT}\right); \quad b_B = b_{B0} \exp\left(\frac{E_B}{RT}\right) \quad \text{(S2)}$$

In eq (S2), E_A and E_B are the energy parameters associated with sites A, and B, respectively.

The isosteric heat of adsorption, Q_{st}, is defined as

$$Q_{st} = -RT^2 \left(\frac{\partial \ln p}{\partial T}\right)_q \quad \text{(S3)}$$

where the derivative in the right member of eq (S3) is determined at constant adsorbate loading, q. The calculations are based on the use of the Clausius-Clapeyron equation.

Breakthrough experiments

The breakthrough experiments were carried out in the dynamic gas breakthrough equipment HPMC-41 (Xuzhou North Gaorui Electronic Equipment Co., Ltd). The experiments were conducted using a stainless steel column (4.9 mm inner diameter × 100 mm length). The weight of ZNU-5 packed in the columns was 0.45g. The column packed with sample was first purged with a Ar flow (5 mL min-1) for 18 h at 60 °C. The mixed gas of C_2H_2/CO_2 (v/v, 50:50), $C_2H_2/CO_2/C_2H_4$ (v/v/v, 33:33:33), and $C_2H_2/CO_2/C_2H_4/CH_4$ (v/v/v/v, 25:25:25:25) was then introduced. All the flowrates are calibrated using the home-made soap-film flowmeter. Outlet gas from the column was monitored using gas chromatography (GC-9860-5CNJ) with the thermal conductivity detector TCD. After the breakthrough experiment, the sample was regenerated with a Ar flow of 5 mL min-1 at 70 °C for 5 h or by desorption under vacuum at 70 °C overnight.

The illustration of the gas breakthrough equipment working mechanism is showing as below: A) under work; B) under purge; C) under vacuum.

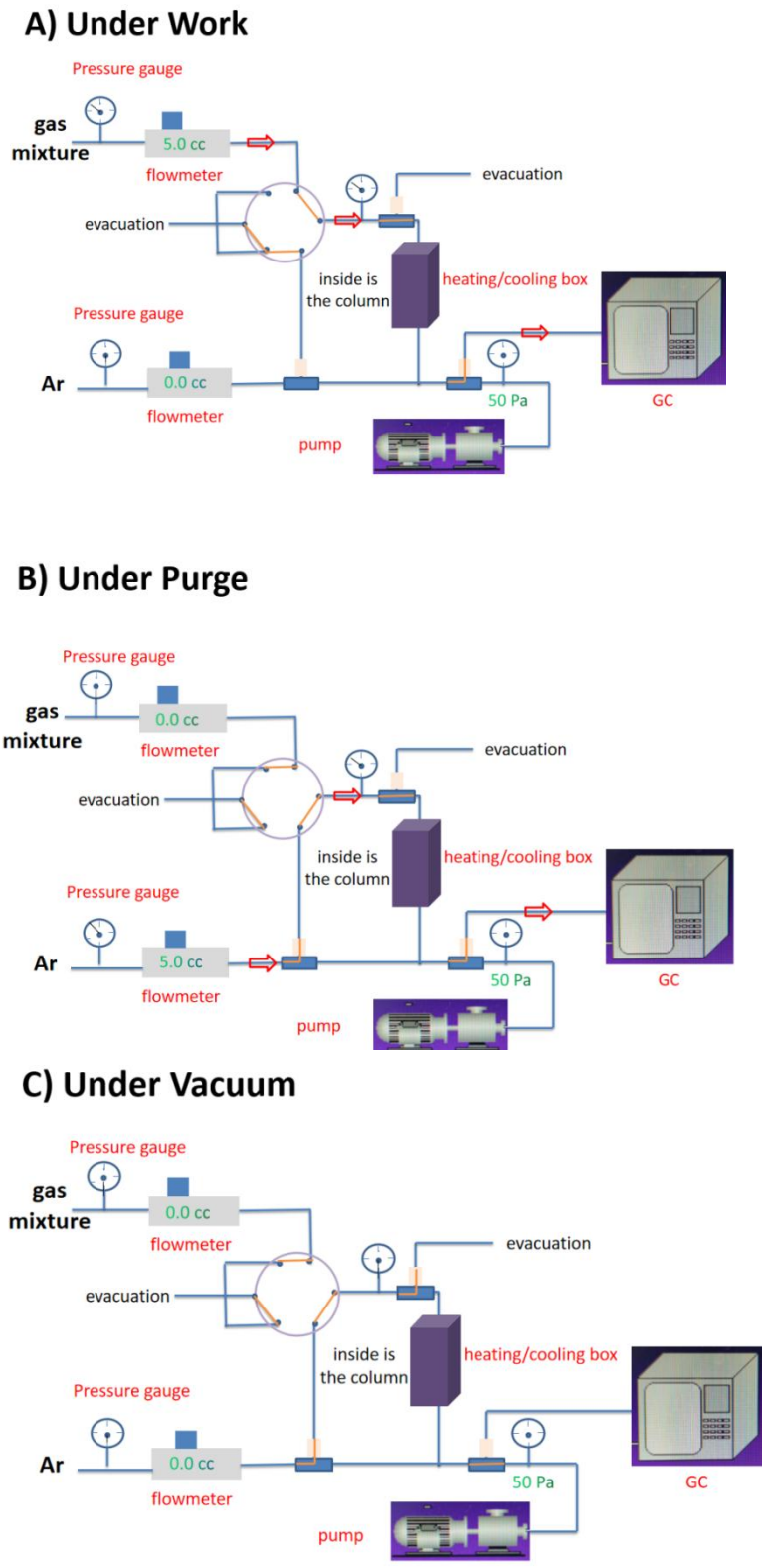

Figure S3 The illustration of the gas breakthrough equipment working mechanism containing gas pipelines, pressure gauge, flowmeter, GC and pump: A) under work, B) under purge, C) under vacuum.

Calculation of separation factor (α)

The amount of gas adsorbed i (qi) is calculated from the breakthrough curves using the following:

$$q_i = \frac{V_T P_i \Delta T}{m} \tag{S4}$$

Here, VT is the total flow rate of gas (mL/min), Pi is the partial pressure of gas i (atm), ΔT is the time for initial breakthrough of gas i to occur (mins) and m is the mass of the sorbent (g). The separation factor (α) of the breakthrough experiment is determined as

$$\alpha = \frac{q_1 y_2}{q_2 y_1} \tag{S5}$$

Where, yi is the partial pressure of gas i in the gas mixture. For equimolar gas mixtures, $y_1=y_2$, $\alpha = q_1/q_2$.

Besides, the separation factor (α) can also be calculated directly from the desorption curves after saturation, where the ratio of areas below the desorption curves is nearly equal to the separation factor.

II. Characterization (SCXRD, PXRD, TGA)

Table S1 Crystallographic data for ZNU-5 and ZNU-4

Materials	**Simulated ZNU-5**	**ZNU-5 immersed to H_2O**	**ZNU-4 (MeCN)**
Cell	a=12.1965(3)	a=12.655(3)	a=18.4836(14)
	b=12.5066(4)	b=12.923(2)	b=17.0872(11)
	c=12.5675(4)	c=14.301(3)	c=11.6222(8)
	α=60.7210(10)	α=63.337(5)	α=90
	β=79.864(2)	β=79.594(6)	β=121.863(2)
	γ=64.958(2)	γ=63.137(5)	γ=90
Temperature	--	193K	193K
Volume(Å3)	--	1863.8(7)	3117.6(4)
Space group	P 1	P -1	C 2/c
Formula	$C_{24}H_{20}CuF_6N_8Ti$	$C_{24}H_{20}CuF_6N_8Ti$	$C_{24}H_{20}CuF_6N_8Ti$, $2(C_2H_3N)$
Mu	-	0.836	1.011
Density	-	1.151	1.551
Z	-	2	4
R	-	0.0847	0.0489
wR2	-	0.2460	0.1221
S	-	0.951	1.048
CCDC No.		2173508	2173507

The single crystals are fragile under normal temperature. Only cell parameters (a,b,c, α, β, γ) can be obtained and the structures are not able to be completely solved unambiguously. Thus, this structure was modified based on its SIFSIX analogue SIFSIX-23-Cu-γ2 (J. Am. Chem. Soc. 2020, 142, 6896-6901). The PXRD pattern from stimulated ZNU-5 is very consistent with that of the as-synthesized ZNU-5.

The single crystals can be perfectly measured at low temperature (eg, 193 K) and solved, but a single crystal to single crystal transformation is observed. The structure solved at 193 K is different from that of synthesized. Interestingly, this newly formed structure is consistent with that of ZNU-5 after immersing to water (Fig. S12B).

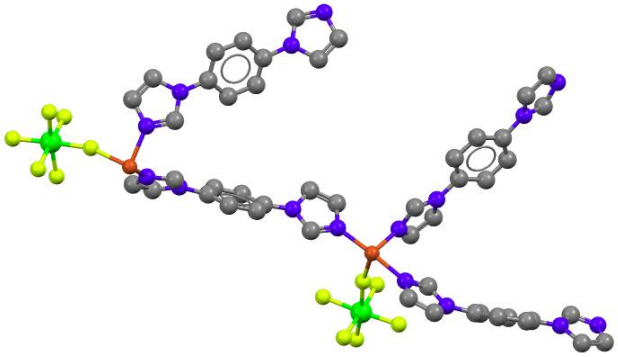

Figure S4 Asymmetric unit of as-synthesized ZNU-5.

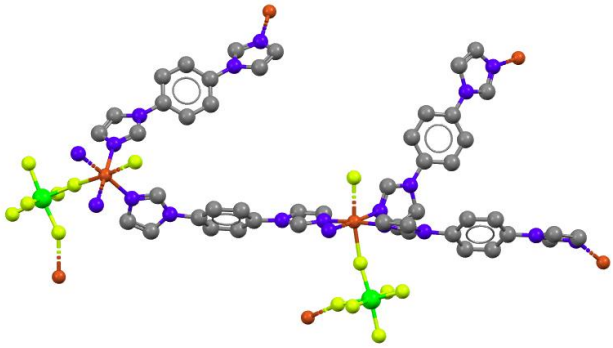

Figure S5 View of the coordination environments of as-synthesized ZNU-5.

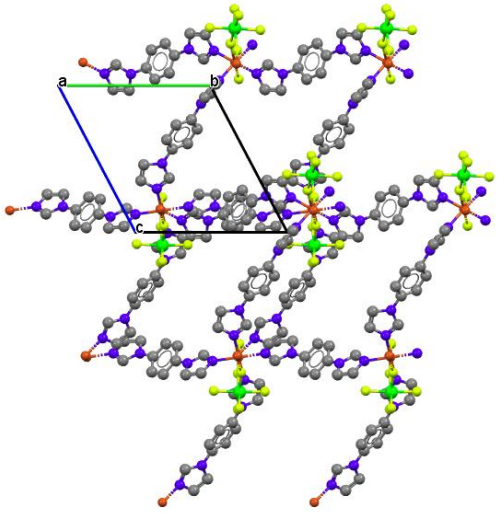

Figure S6 Single crystal structure of as-synthesized ZNU-5 viewed along axis a.

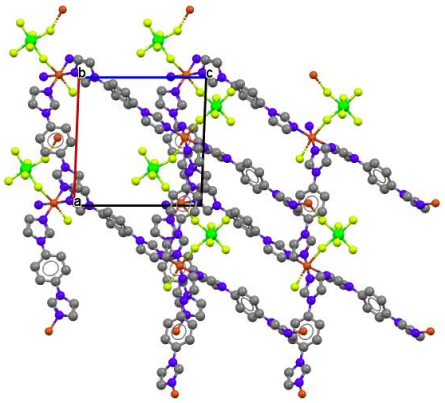

Figure S7 Single crystal structure of as-synthesized ZNU-5 viewed along axis b.

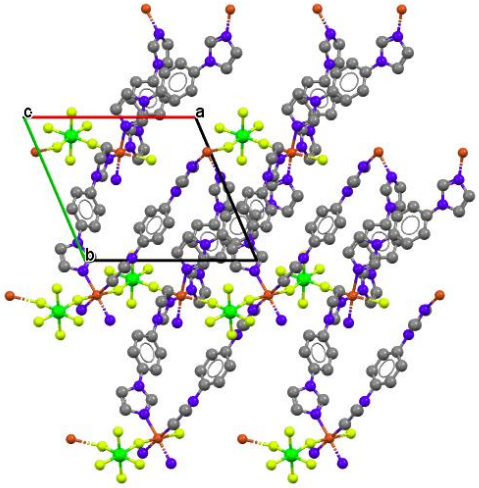

Figure S8 Single crystal structure of as-synthesized ZNU-5 viewed along axis c.

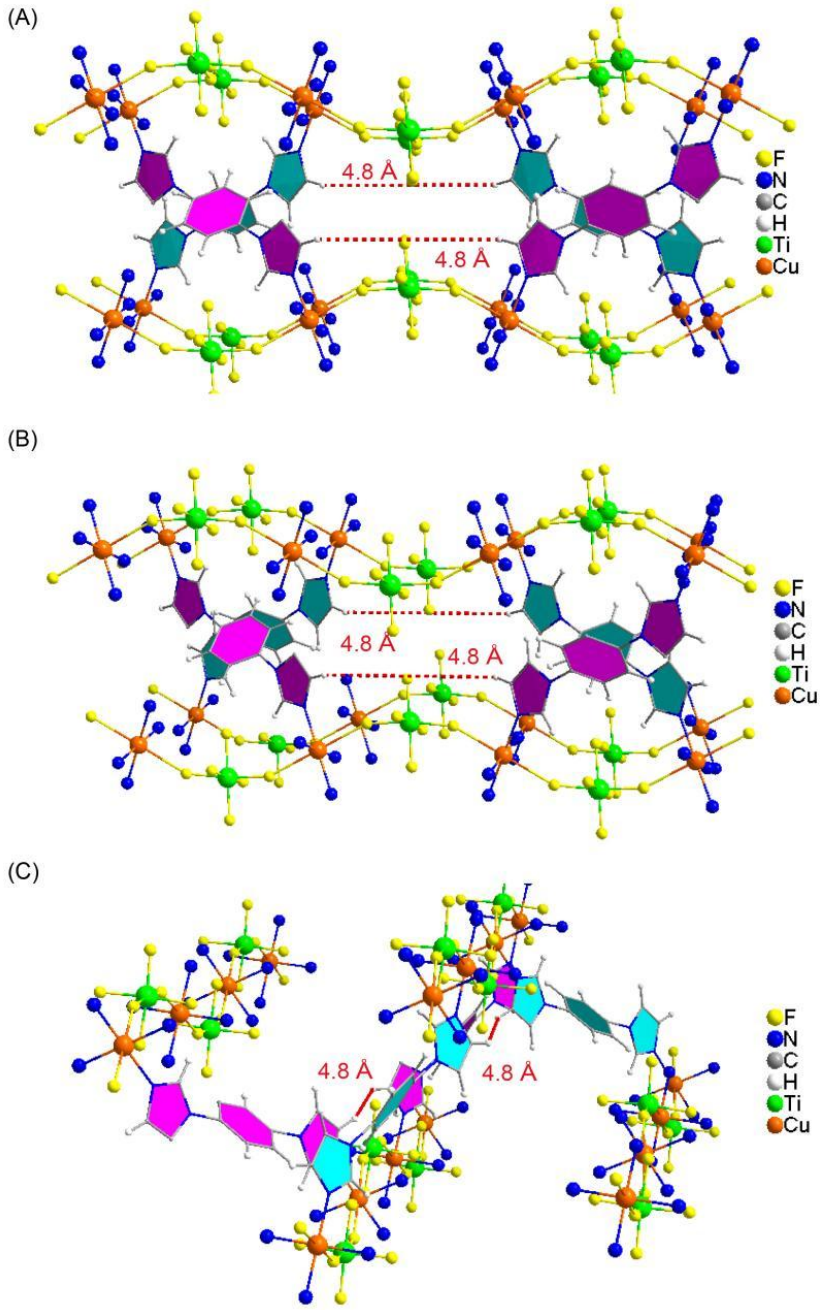

Figure S9 Crystal structures of ZNU-4 shown in different directions for the demonstration of the pore size. The distances have subtracted the the Van der Waal radii of the two hydrogen atoms.

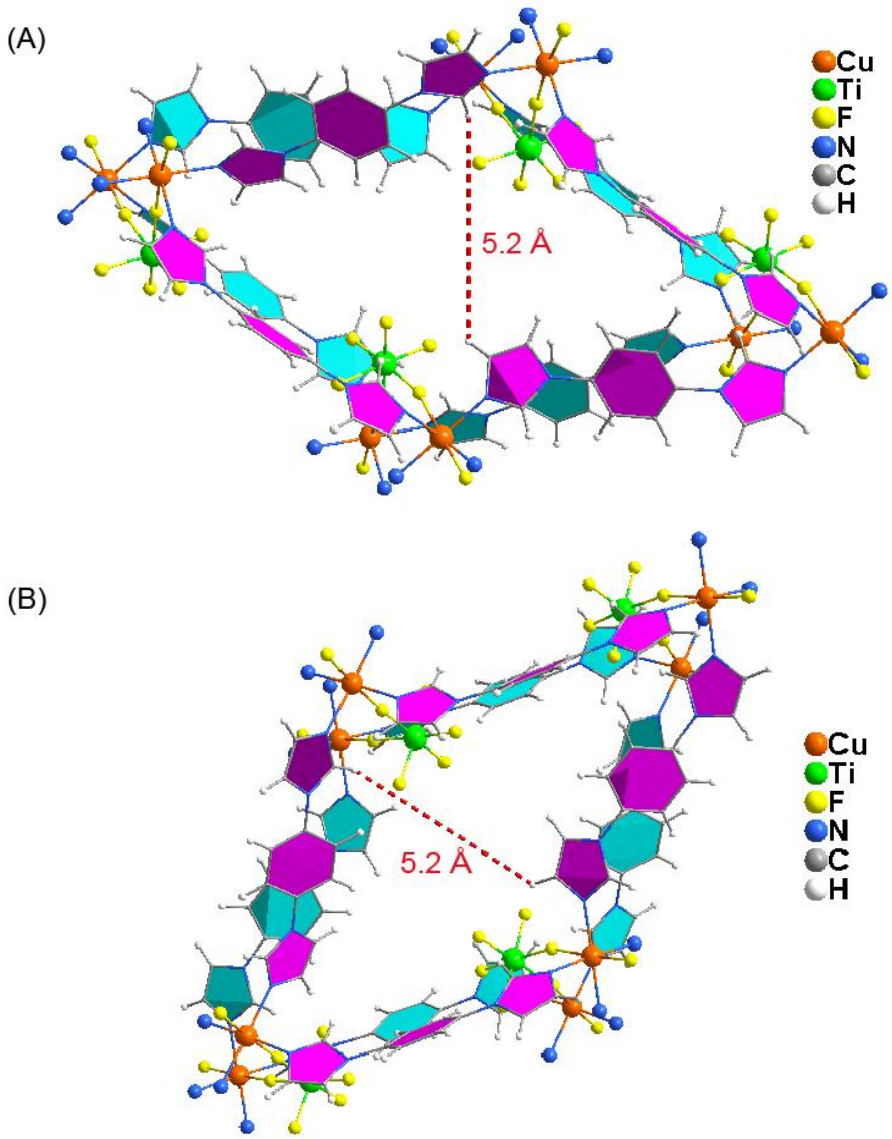

Figure S10 Crystal structures of as-synthesized ZNU-5 shown in different directions for the demonstration of the pore size. The distances have subtracted the the Van der Waal radii of the two hydrogen atoms.

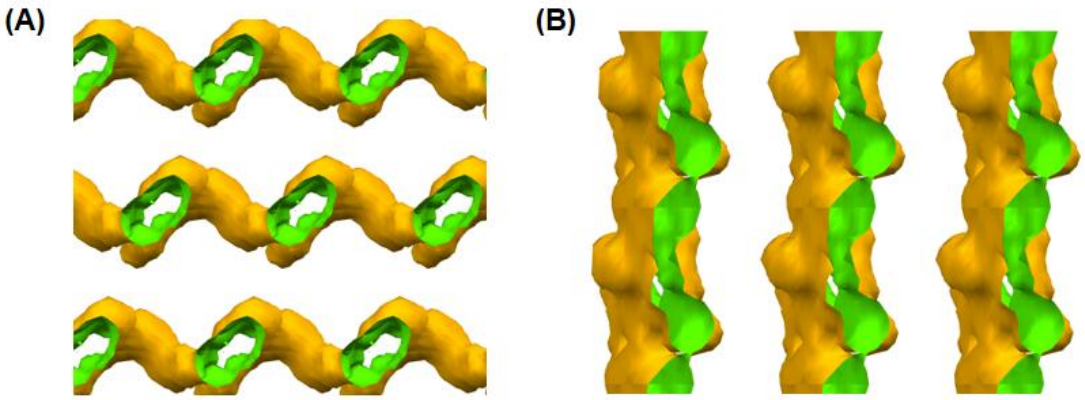

Figure S11 Voids of as-synthesized ZNU-5 viewed along the crystallographic axis a(A) and b(B).

Table S2 Comparison of the physical properties of C_2H_2, CO_2 ,C_2H_4 ,and CH_4

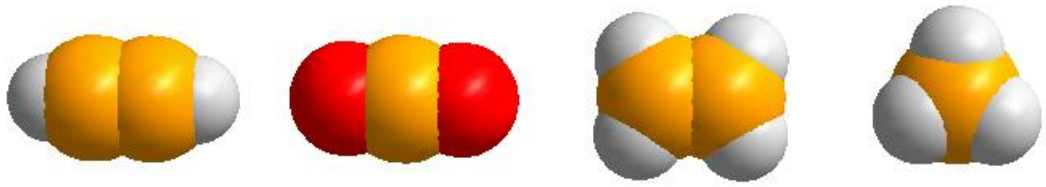

Molecular formula	Molecular dimension(Å)			Kinetic diameter(Å)	Polarizability ×10-25(cm^3)	Boiling point (K)
	X	Y	Z			
C_2H_2	3.32	3.34	5.70	3.33	33.3-39.3	188.4
CO_2	3.18	3.33	5.36	3.33	29.11	194.7
C_2H_4	3.28	4.18	4.84	4.16	42.5	169.4
CH_4	3.83	3.94	4.10	3.76	25.93	111.7

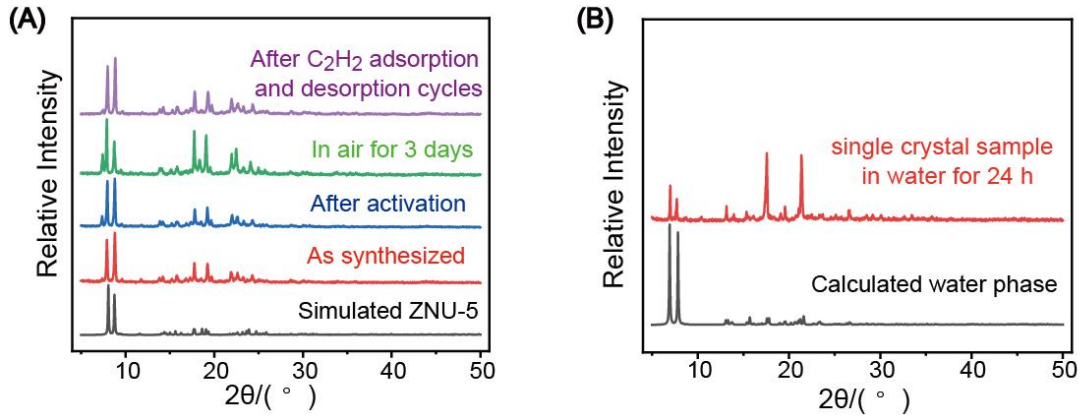

Figure S12 PXRD patterns of ZNU-5 under different condition.

Analysis: PXRD patterns revealed that there are minor differences between the activated samples and the as-synthesized samples. Such small differences are often found in many reported materials and regarded as the complete retention of the original structures. Take some for examples: NTU-55 (ACS Appl. Mater. Interfaces. 2020, 12, 3764−3772) , PCP-31 (J. Am. Chem. Soc. 2017, 139, 11576−11583) , UTSA-222 (Inorg. Chem. 2017, 56, 7145−7150), and ZJU-8 (RSC Adv. 2015, 5, 77417−77422). Besides, slight bond length and angle changes are also very common after the removal of the guests. In our case, the framework is very flexible. After the guest molecules are removed, the framework must have slight bond length and angle changes, which is reflected by the slight difference of PXRD patterns as well as its gate opening behavior for gas adsorption. This small changes are very difficult to characterize by single crystal XRD.

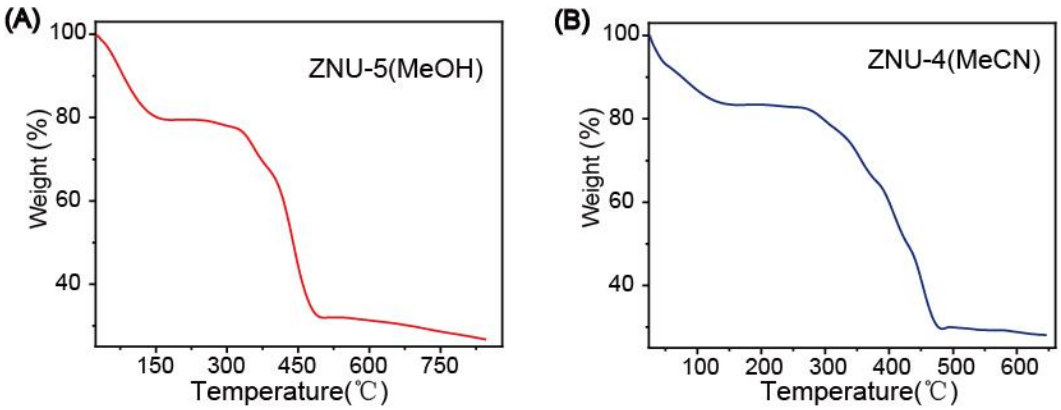

Figure S13 Thermogravimetric analysis curve of ZNU-4 and ZNU-5.

III. Adsorption data

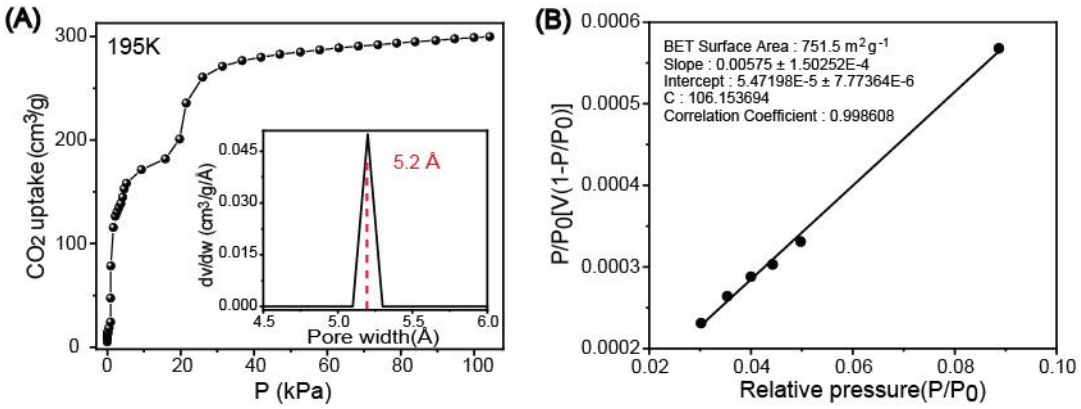

Figure S14 (A) CO_2 adsorption isotherm for ZNU-5 at 195 K and its calculated pore size distribution.(B) BET surface area plot of ZNU-5.

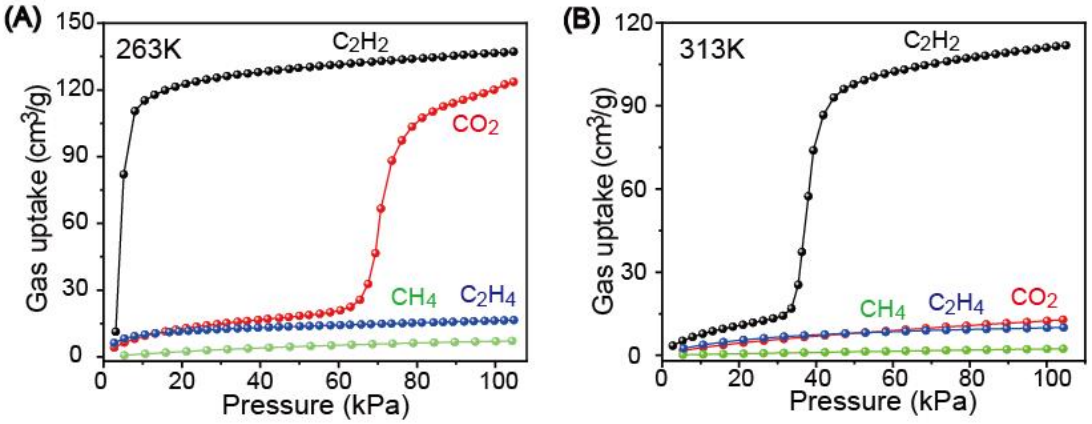

Figure S15 The sorption isotherm of C_2H_2 , CO_2, C_2H_4, and CH_4 on ZNU-5 at 263K (A) and 313 K (B).

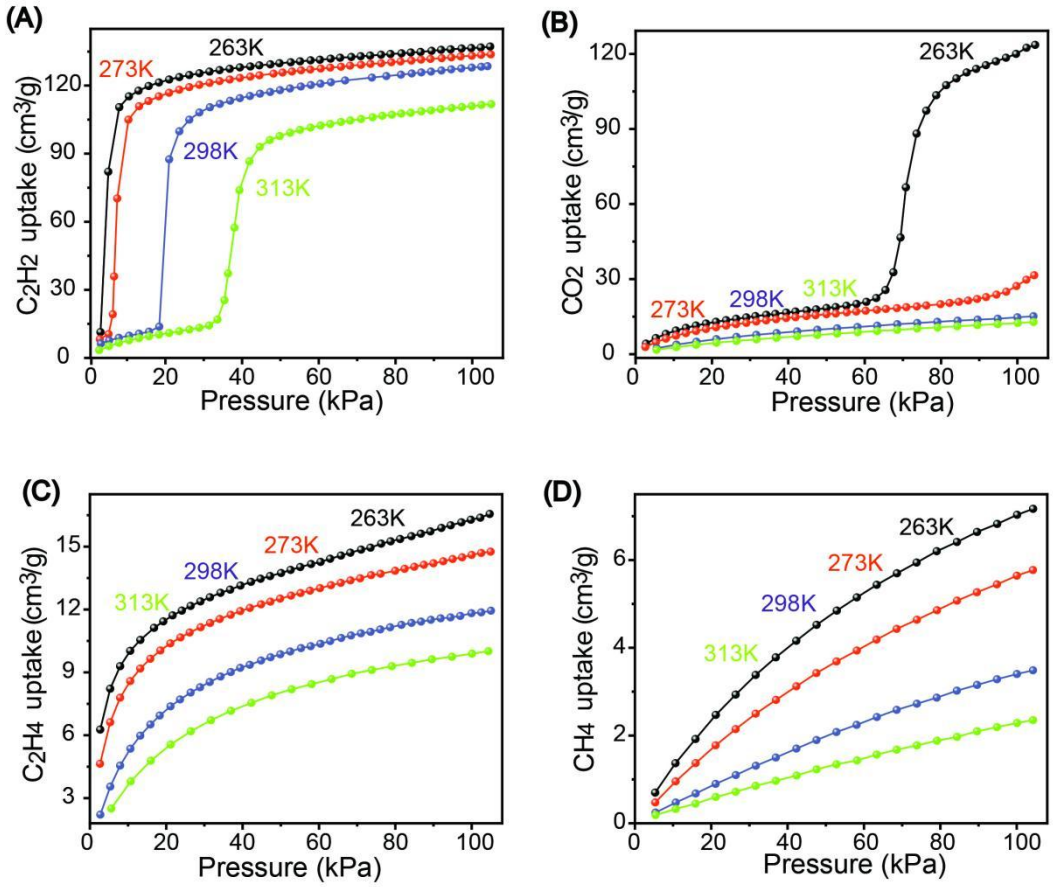

Figure S16 The sorption isotherm of C_2H_2 , CO_2, C_2H_4, and CH_4 on ZNU-5 at different temperature.

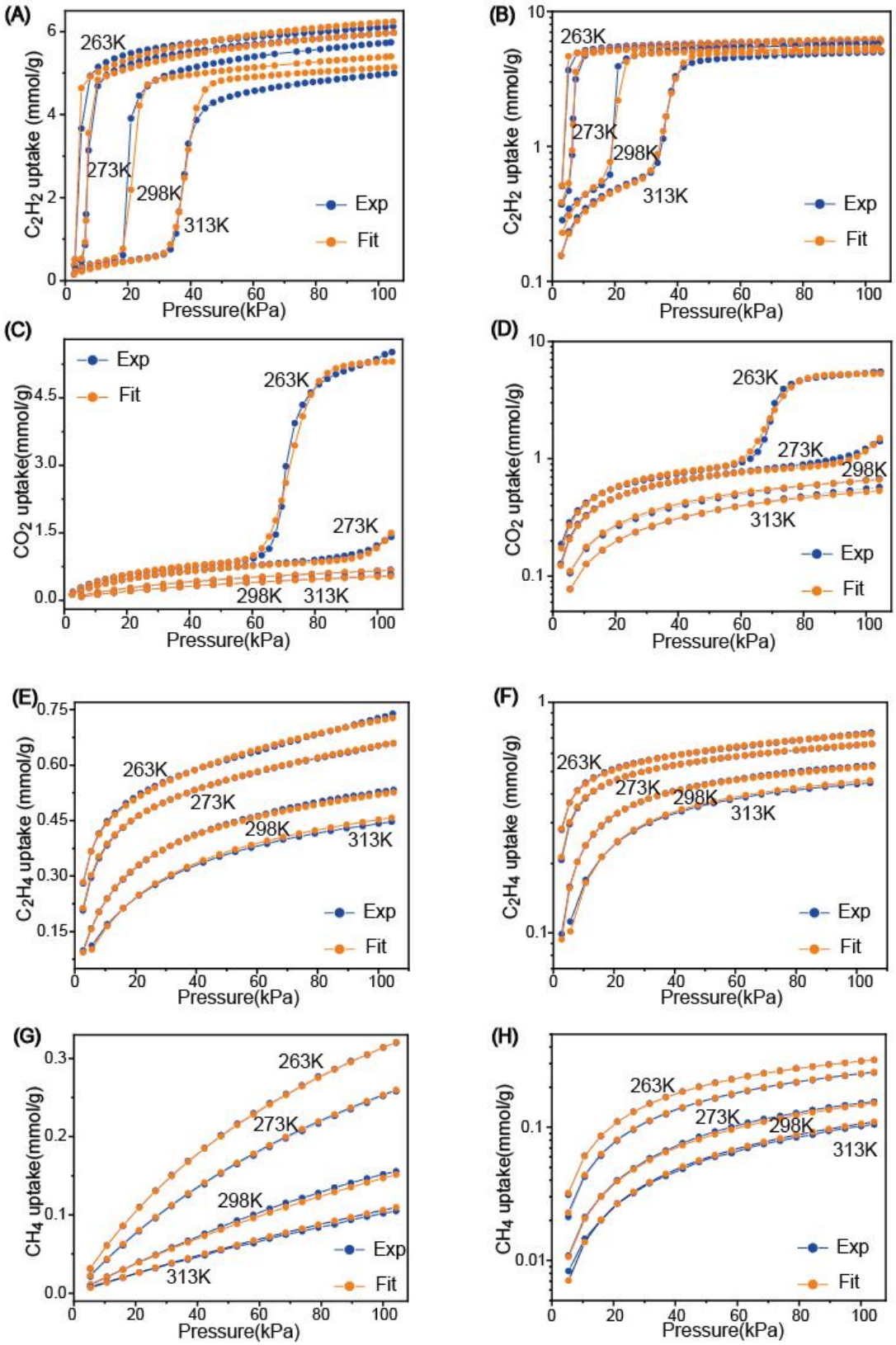

Figure S17 Experimental and DSLF fitting adsorption isotherms of C_2H_2, CO_2, C_2H_4, and CH_4 On ZNU-5 at 263K, 273K, 298K, and 313K.

Table S3 Dual-site Langmuir-Freundlich fits for C_2H_2, CO_2, C_2H_4 and CH_4 in ZNU-5

	Site A				Site B			
Parameter	$q_{A,sat}$	B_{A0}	E_A	V_A	$q_{B,sat}$	B_{B0}	E_B	V_B
unit	mol kg^{-1}	Pa^{-VA}	kJ mol-1	--	mol kg-1	Pa^{-VB}	kJ mol^{-1}	--
C_2H_2	4.1	1.806E-190	593	19.8	3.83	5.927E-07	16.7	0.6
CO_2	4.3	1.965E-205	545	19.85	1.4	3.063E-08	19.7	0.8
C_2H_4	0.62	5.541E-11	25.6	1	0.48	1.868E-10	32.3	1
CH_4	2.4	1.226E-12	26.5	1	0.47	7.671E-10	21.2	1

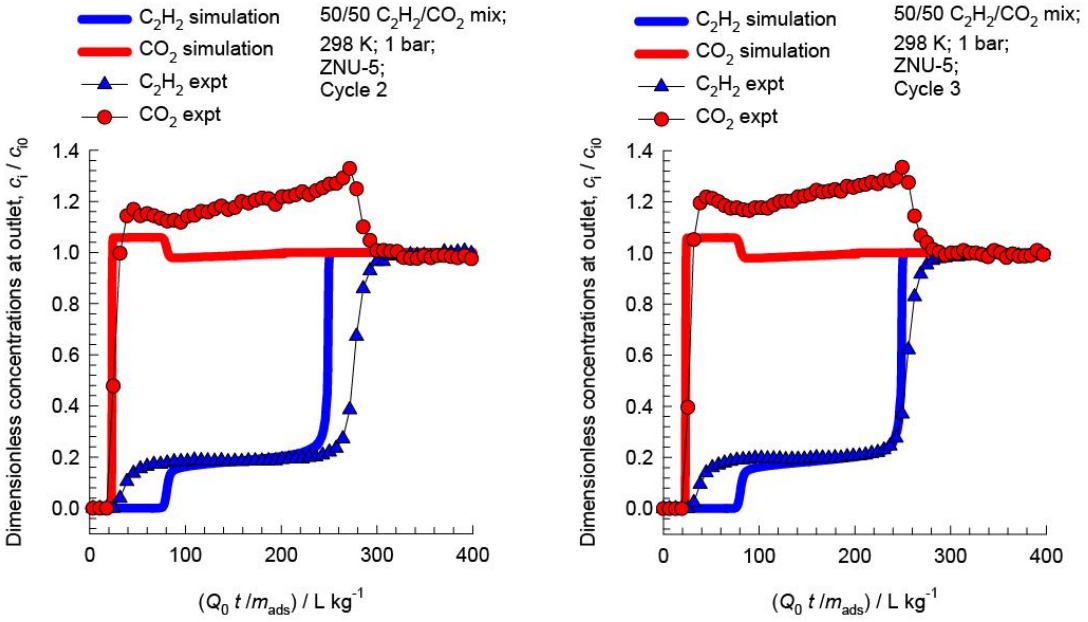

Figure S18 Simulated and Experimental breakthrough curves of C_2H_2/CO_2(50/50) at 298K for the thired cycle.

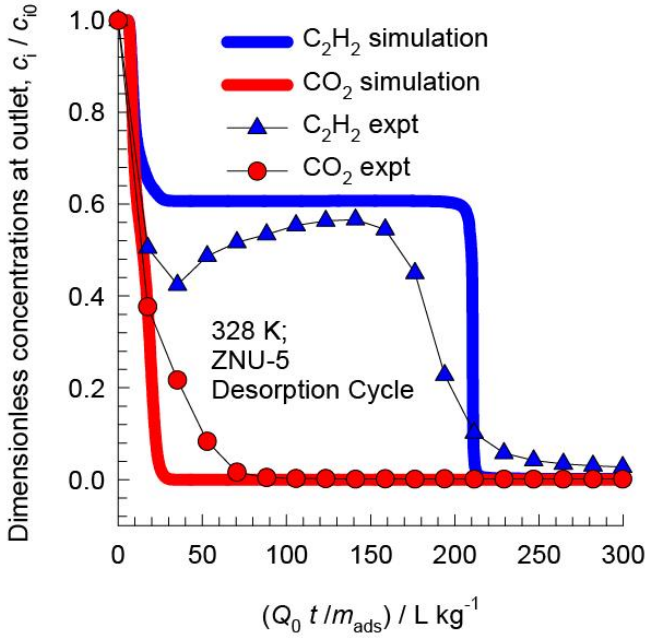

Figure S19 Simulated and Experimental desorption curves after the breakthrough experiment of C_2H_2/CO_2(50/50) mixtures under a constant Ar flow rate of 5 mL/min at 328 K and 1.0 bar .

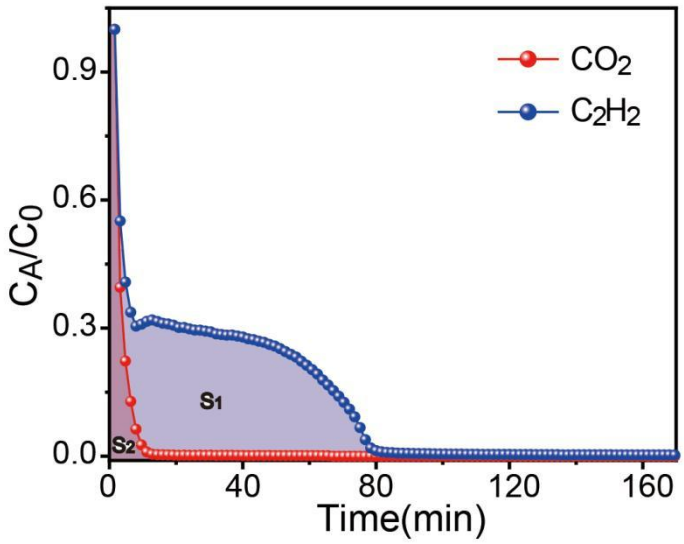

Figure S20 Experimental desorption curves after the breakthrough experiment of C_2H_2/CO_2 (50/50, v/v) mixtures under a constant Ar flow rate of 5 mL/min at 298 K and 1.0 bar.

Calculation of the area of the C_2H_2 and CO_2 area indicates the separation factor of C_2H_2/CO_2 (50/50, v/v) by ZNU-5 is ~9.1.

IV Comparison Table

Table S4 Comparison of the reported materials on C_2H_2/CO_2 adsorption capacity, IAST selectivity towards C_2H_2/CO_2 and C_2H_2/CO_2 adsorption enthalpy (Qst)

Adsorbents	Surface area ($m^2 \cdot g^{-1}$, BET)	C_2H_2 uptake ($cm^3 \cdot g^{-1}$)	CO_2 uptake ($cm^3 \cdot g^{-1}$)	Uptake ratio	IAST (C_2H_2/CO_2) (50/50)	Qst (C_2H_2 kJ·mol^{-1})	Qst (CO_2 kJ·mol^{-1})	Ref
C2H2/CO2 adsorption by molecular sieving mechanism								
ZNU-5	751.5	128.6	15.2	8.5	12	27.8	-	This work
UTSA-300	311	69.0	3.36	20.5	743	57.6	-	[1]
CPL-1-NH_2	103	41.2	4.70	8.8	119	50.0	33.0	[2]
ZNU-3	463	81.0	5.44	14.9	-	23.4	-	[3]
ZJU-196a	-	83.5	8.50	9.8	-	39.2	-	[4]
SIFSIX-dps-Cu	358	102.4	13.7	7.5	1786.6	60.5	-	[5]
GeFSIX-dps-Cu	310	90.5	10.1	9.0	171.9	56.3	-	[5]
NTU-65	680	75.3	2.3	33.6	-	-	-	[6]
C2H2/CO2 adsorption by thermodynamic mechanism								
ZNU-4	358.6	85.1	44.0	1.9	8.9	50.28	34.57	This work
ZNU-1	532	76.3	38.1	2.0	56.6	54.0	44.0	[7]
BSF-1	535	52.6	39.7	1.3	3.3	31	22	[8]
BSF-2	403	41.4	29.8	1.4	5.1	37.3	28.7	[9]
BSF-3	485	80.4	47.3	1.7	16.3	42.7	22.4	[10]
BSF-4	437	53.3	35.8	1.5	9.8	35	-	[11]
PCP-31	2858	50.0	34.9	1.4	43	53	30	[12]
PCP-32	4856	84.9	34.9	2.4	23	36	26	[12]
PCP-33	1248	121.8	58.7	2.1	6	27.5	26	[13]
UTSA-50[a]	604	90.5	64.5	1.4	13.3	39.4	27.8	[14]
UTSA-68[a]	2501	70.1	39.6	1.8	3.3	25.8	-	[15]
UTSA-74a	830	108.0	63.9	1.7	9	32	25	[16]
UTSA-98	1400	82.6	40.3	2.0	5.2	22.8	18.3	[17]

UTSA-220	577	76.2	75.7	1.0	4.4	29	27	[18]
UTSA-222a[a]	703	85.3	42.8	2.0	2	26	17	[19]
iMOF-5C	242	32.5	14.6	2.2	6	35.5	-	[20]
iMOF-6C	330	24.9	21.3	1.2	8	38	-	[20]
iMOF-7C	109	15.7	13.7	1.1	4	35	-	[20]
JCM-1	550	75.0	38.1	2.0	13.7	36.9	33.4	[21]
SIFSIX-Cu-TPA	1330	185.2	107.3	1.1	5.3	39.1	25.7	[22]
SIFSIX-21-Ni	871	90.0	29.1	3.1	27.7	37.9	19.8	[23]
TIFSIX-2-Ni-i	480.5	94.3	101.6	0.9	6.1	40	34	[24]
TIFSIX-2-Cu-i[c]	685	91.8	96.3	1.0	6.5	46.3	35.8	[24]
MPM-1-TIFSIX	950	101.5	86.9	1.2	0.83	30.1	48.4	[25]
SIFSIX-17-Ni	229.2	74.0	51.5	44.2	40.2	1.44	11.7	[26]
TIFSIX-17-Ni	237.6	73.0	47.0	48.3	37.8	1.55	20.9	[26]
UPC-110	1384.3	73.4	24.2	3.0	5.1	24.6	13	[27]
MUF-15[b]	1130	109.1	84.7	1.3	4.2	24.2	28.3	[28]
MUF-17[b]	247	61.2	51.1	1.2	6.01	49.5	31.1	[29]
TCuI	250	49.3	35.8	1.4	5.3	38.4	26.6	[30]
TCuBr	173	62.7	44.8	1.4	9.5	36.6	30.2	[30]
TCuCl	167	67.2	44.8	1.5	16.9	41	30.1	[30]
CAU-10-H[a]	627	89.8	60.0	1.5	4	27	25	[31]
CAU-10-NH_2	403	96.3	56.0	1.7	10.8	31.3	24.5	[32]
MIL-160	1138	190.8	90.0	2.1	10	31.8	26.9	[33]
CAU-23	1320	119.0	71.9	1.7	3.8	26.7	20	[33]
MOF-NH_2	120	60.0	31.4	1.9	12.6	16.7	24.2	[34]
MOF-OH	150	68.1	26.9	2.5	25	17.5	20.6	[34]
SNNU-37(Fe)	293.1	108.9	47.7	2.3	9.9	35	33.6	[35]
SNNU-37(Sc)	297.6	78.2	34.0	2.3	2.7	34.4	33.4	[35]
SNNU-45	1007	134.0	97.4	1.4	8.5	39.9	27.1	[36]
SNNU-63	1719.8	91.1	43.7	2.1	3.3	21.6	21.95	[37]
SNNU-65-Cu-Sc	2089.2	179.0	70.3	2.5	13.5	44.9	22.2	[38]
SNNU-65-Cu-Fe	2112	162.4	65.0	2.5	6.7	28.2	21.8	[38]
SNNU-65-Cu-Ga	1918	141.6	58.7	2.4	18.7	31.7	20.5	[38]

SNNU-65-Cu-In	1936.2	153.2	56.0	2.7	7	23.4	24.9	[38]
SNNU-150-Al	-	97.0	44.4	2.2	7.27	29	24.8	[39]
SNNU-150-Ga	-	39.9	26.7	1.5	4.93	33	28	[39]
SNNU-150-In	-	34.9	23.1	1.5	5.57	36	32	[39]
ZJU-60[a]	1627	150.6	73.3	2.1	6.7	17.6	15.2	[40]
ZJU-74[a]	694	85.7	69.0	1.2	36.5	44.5	30	[41]
ZJU-199[a]	987	128.0	62.4	2.1	4	38.5	29	[42]
ZJUT-2[a]	-	76.0	49.0	1.6	10	41.5	36.1	[43]
PCM-48[a]	300	25.5	21.7	1.2	4.3	23.6	15.4	[44]
JXNU-12	2544	78.0	37.4	2.1	2	21.3	19.9	[45]
JXNU-12(F)	2154	115.6	33.4	3.5	4.1	28	19.7	[45]
NbU-8[b]	1467.4	190.4	49.3	3.9	5	34.6	30.3	[46]
NbU-10[b]	292	45.0	31.0	1.5	6.5	34.6	27.6	[47]
FJU-6-TATB[a]	731	110.0	58.0	1.9	3.1	29	26	[48]
FJU-89a	774	101.5	61.2	1.7	4.3	31	27.8	[49]
FJU-90a	1572	180.1	103.0	1.7	4.3	25.1	20.7	[50]
ZJU-195	1721.9	214.2	105.0	2.0	4.7	29.9	20.7	[51]
CuI@UiO-66-$(COOH)_2$	302.3	51.5	19.9	2.6	73	74.5	28.9	[52]
Cu-CPAH	880	131.7	88.0	1.5	3.6	35.4	31.5	[53]
FeNi-M'MOF	383	96.1	60.9	1.6	24	27	24.5	[54]
NKMOF-1-Ni	382	60.9	51.1	1.2	25	60.3	40.9	[55]
IPM-101	343	57.1	68.1	0.8	12.3	43.7	30.7	[56]
DICRO-4-Ni-i	398	43.0	23.1	1.9	13.9	37.7	33.9	[57]
CPM-107op	319	97.4	35.0	2.8	5.7	32	24	[58]
$[Ni_3(HCOO)_6]$	288.6	53.3	38.8	1.4	22	40.9	24.5	[59]
NTU-54[e]	-	22.0	19.0	1.2	6.3	38	35	[60]
NTU-55	2300	140.4	65.0	2.2	4.5	25.5	22	[61]
NTU-66-Cu	1700	111.6	49.1	2.3	6	32.3	21.7	[62]
HOF-3[a]	165	47.0	21.1	2.2	21	42	19	[63]
$[Ni(dpip)]\cdot 2.5DMF\cdot H_2O$	553.8	83.6	58.7	1.4	1.9	41.7	30.3	[64]
[Ni(tzba)0.5(F)(bpy)]	700	125.0	85.1	1.5	3	36.7	25.6	[65]
M′ MOF-2a[d]	598	43.9	30.0	1.5	1.89	32.7	32.5	[66]

M′ MOF-3a[d]	237	42.1	10.1	4.2	8.41	27.3	40.5	[66]
$Cu_2(ade)_2(PA)_2$	401	49.1	33.6	1.5	4.1	26.8	23.6	[67]
JNU-1	818	63.0	51.0	1.2	3	13	-	[68]
JNU-2	1144	102.8	49.5	2.1	3.5	15.8	13.5	[68]
UPC-200(Al)-F-BIM	3192	139.8	54.7	2.6	2.25	20.5	14	[69]
SDU-CP-1[c]	1986.5	84.9	38.1	2.2	2.5	27.9	21.4	[70]
MPM-1-Cl	491	67.9	43.0	1.6	3.21	27.3	23.1	[71]
$Ca(dtztp)_{0.5}(DMA)]\cdot 2H_2O$	553.8	110.0	93.6	1.2	1.8	28.8	19.2	[72]
Cu(BDC-Br)	303	34.3	24.2	1.4	3.9	26.1	25.6	[73]
JXNU-5a	406	55.9	34.8	1.6	5	32.9	25.2	[74]
ATC-Cu	600	112.2	90.0	1.2	53.6	79.1	-	[75]
FJU-22a	828.2	114.8	111.3	1.03	-	23	-	[76]
FJU-36	409	52.2	35.5	1.5	2.8	32.9	31.1	[77]
ZJU-195	1721.9	214.2	105.0	2.0	4.7	29.9	20.7	[78]
ZJNU-13	1352	118.4	87.9	1.3	5.64	33.5	22.5	[79]
$[Ni_2(BTEC)(bipy)_3]$	97	76.8	13.0	5.9	33.5	19.8	25	[80]
$Zn_2(Pydc)(Ata)_2$	636	47.2	33.0	1.4	3.9	43.1	32.1	[81]
MAF-2	-	70.1	19.04	3.7	-	29.8	25.8	[82]
sql-16-Cu-NO_3	-	34.7	16.7	2.1	78	38.6	25.6	[83]

a: At temperature of 296 K

b: At temperature of 293 K

c: IAST(C_2H_2/CO_2=2:1)

d: At temperature of 295 K

e: At temperature of 273 K

Supplementary References

[1] Lin, R.-B.; Li, L.; Wu, H.; Arman, H.; Li, B.; Lin, R.-G.; Zhou, W.; Chen, B. Optimized Separation of Acetylene from Carbon Dioxide and Ethylene in a Microporous Material. *J. Am. Chem. Soc*. **2017**, *139*, 8022-8028.

[2] Yang, L.; Yan, L.; Wang, Y.; Liu, Z.; He, J.; Fu, Q.; Liu, D.; Gu, X.; Dai, P.; Li, L.; Zhao, X. Adsorption Site Selective Occupation Strategy within a Metal-Organic Framework for Highly Efficient Sieving Acetylene from Carbon Dioxide. *Angew. Chem. Int. Ed*. **2021**, *60*, 4570-4574.

[3] Sun, W.-Q.; Hu, J.-B.; Jiang, Y.-J.; Xu, N.; Wang, L.-Y.; Li, J.-H.; Hu, Y.-Q.; Duttwyler, S.; Zhang, Y.-B. Flexible molecular sieving of C_2H_2 from CO_2 by a new cost-effective metal organic framework with intrinsic hydrogen bonds. *Chem. Eng. J.* **2022**, *439*, 135745.

[4] Zhang, L.; Jiang, K.; Li, L.; Xia, Y.-P. Hu, T.-L.; Yang, Y.; Cui, Y.; Li, B.; Chen. B.; Qian, G. Efficient separation of C_2H_2 from C_2H_2/CO_2 mixtures in an acid-base resistant metal-organic framework. *Chem. Commun*. **2018**, *54*, 4846-4849.

[5] Wang, J.; Zhang, Y.; Su, Y.; Liu, X.; Zhang, P.; Lin, R.-B.; Chen, S.; Deng, Q.; Zeng, Z.; Deng, S.; Chen. B. Fine pore engineering in a series of isoreticular metal-organic frameworks for efficient C_2H_2/CO_2 separation. *Nat. Commun*. **2022**, *13*, 200.

[6] Dong, Q.; Zhang, X.; Liu, S.; Lin, R.-B.; Guo, Y.; Ma, Y.; Yonezu, A.; Krishna, R.; Liu, G.; Duan, J.; Matsuda, R.; Jin, W.; Chen, B. Tuning Gate-Opening of a Flexible Metal-Organic Framework for Ternary Gas Sieving Separation. *Angew. Chem. Int. Ed*. **2020**, *59*, 22756-22762.

[7] Wang, L.; Sun, W.; Zhang, Y.; Xu, N.; Krishna, R.; Hu, J.; Jiang, Y.; He, Y.; Xing, H. Interpenetration Symmetry Control Within Ultramicroporous Robust Boron Cluster Hybrid MOFs for Benchmark Purification of Acetylene from Carbon Dioxide. *Angew. Chem. Int. Ed*. **2021**, *60*, 22865-22870.

[8] Zhang, Y.; Yang, L.; Wang, L.; Duttwyler, S.; Xing, H. A Microporous Metal-Organic Framework Supramolecularly Assembled from a CuII Dodecaborate Cluster Complex for Selective Gas Separation. *Angew. Chem. Int. Ed*. **2019**, *58*, 8145-8150.

[9] Zhang, Y.; Yang, L.; Wang, L.; Cui, X.; Xing, H. Pillar iodination in functional boron cage hybrid supramolecular frameworks for high performance separation of light hydrocarbons. *J. Mater. Chem. A*. **2019**, *7*, 27560-27566.

[10] Zhang, Y.; Hu, J.; Krishna, R.; Wang, L.; Yang, L.; Cui, X.; Duttwyler, S.; Xing, H. Rational Design of Microporous MOFs with Anionic Boron Cluster Functionality and Cooperative Dihydrogen Binding Sites for Highly Selective Capture of Acetylene. *Angew. Chem. Int. Ed.* **2020**, *59*, 17664-17669.

[11] Zhang, Y.; Wang, L.; Hu, J.; Duttwyler, S.; Cui X.; Xing H. Solvent-dependent supramolecular self-assembly of boron cage pillared metal-organic frameworks for selective gas separation. *CrystEngComm*. **2020**, *22*, 2649-2655.

[12] Duan, J.; Higuchi, M.; Zheng, J.; Noro, S.-I.; Chang, I-Y.; Hyeon-Deuk, K.; Mathew, S.; Kusaka, S.; Sivaniah, E.; Matsuda, R.; Sakaki, S.; Kitagawa, S. Density Gradation of Open Metal Sites in the Mesospace of Porous Coordination Polymers. *J. Am. Chem. Soc*. **2017**, *139*, 11576−11583.

[13] Duan, J.; Jin, W.; Krishna. R. Natural Gas Purification Using a Porous Coordination Polymer with Water and Chemical Stability. *Inorg. Chem*. **2015**, *54*, 4279−4284.

[14] Xu, H.; He, Y.; Zhang, Z.; Xiang, S.; Cai, J.; Cui, Y.; Yang, Y.; Qian, G.; Chen, B. A microporous metal-organic framework with both open metal and Lewis basic pyridyl sites for highly selective C_2H_2/CH_4 and C_2H_2/CO_2 gas separation at room temperature. *J. Mater. Chem. A*. **2013**, *1*, 77-81.

[15] Chang, G.; Li, B.; Wang, H.; Hu, T.; Bao, Z.; Chen, B. Control of interpenetration in a microporous metal-organic framework for significantly enhanced C_2H_2/CO_2 separation at room temperature. *Chem. Commun*. **2016**, *52*, 3494-3496.

[16] Luo, F.; Yan, C.; Dang, L.; Krishna, R.; Zhou, W.; Wu, H.; Dong, X.; Han, Y.; Hu, T.-L.; O'Keeffe, M.; Wang, L.; Luo, M.; Lin, R.-B.; Chen. B. UTSA-74: A MOF-74 Isomer with Two Accessible Binding Sites per Metal Center for Highly Selective Gas Separation. *J. Am. Chem. Soc*. **2016**, *138*, 5678-5684.

[17] Wang, X.; Wang, B.; Zhang, X.; Xie, Y.; Arman, H.; Chen, B. A Copper-Based Metal-Organic Framework for C_2H_2/CO_2 Separation. *Inorg. Chem.* **2021**, *60*, 18816-18821.

[18] Li, H.; Li, L.; Lin, R.-B.; Ramirez, G.; Zhou, W.; Krishna, R.; Zhang, Z.; Xiang, S.; Chen, B. Microporous Metal-Organic Framework with Dual Functionalities for Efficient Separation of Acetylene from Light Hydrocarbon Mixtures. *ACS Sustaina. Chem. Eng*. **2019**, *7*, 4897-4902.

[19] Ma, J.-X.; Guo, J.; Wang, H.; Li, B.; Yang, T.; Chen. B. Microporous Lanthanide Metal-Organic Framework Constructed from Lanthanide Metalloligand for Selective Separation of C_2H_2/CO_2 and C_2H_2/CH_4 at Room Temperature. *Inorg. Chem*. **2017**, *56*, 7145-7150.

[20] Dutta, S.; Mukherjee, S.; Qazvini, O. T.; Gupta, A. K.; Sharma, S.; Mahato, D.; Babarao, R.; Ghosh, S. K. Three-in-One C_2H_2-Selectivity-Guided Adsorptive Separation across an Isoreticular Family of Cationic Square-Lattice MOFs. *Angew. Chem. Int. Ed*. **2022**, *61*, e202114132.

[21] Lee, J.; Chuah, C. Y.; Kim, J.; Kim, Y.; Ko, N.; Seo, Y.; Kim, K.; Bae, T. H.; Lee, E. Separation of Acetylene from Carbon Dioxide and Ethylene by a Water-Stable Microporous Metal-Organic Framework with Aligned Imidazolium Groups inside the Channels. *Angew. Chem. Int. Ed*. **2018**, *57*, 7869-7873.

[22] Li, H.; Liu, C.; Chen, C.; Di, Z.; Yuan, D.; Pang, J.; Wei, W.; Wu, M.; Hong, M. An Unprecedented Pillar-Cage Fluorinated Hybrid Porous Framework with Highly Efficient Acetylene Storage and Separation. *Angew. Chem. Int. Ed.* **2021**, *60*, 7547-7552.

[23] Kumar, N.; Mukherjee, S.; Harvey-Reid, N. C.; Bezrukov, A. A.; Tan, K.; Martins,V.; Vandichel, M.; Pham, T.; Wyk, L. M. V.; Oyekan, K.; Kumar, A.; Forrest, K. A.; Patil, K. M.; Barbour, L. J.; Space, B.; Huang, Y.; Kruger, P. E.; Zaworotko, M. J. Breaking the trade-off between selectivity and adsorption capacity for gas separation. *Chem*. **2021**, *7*, 3085-3098.

[24] Jiang, M. D.; Cui, X.; Yang, L.; Yang, Q.; Zhang, Z.; Yang, Y.; Xing, H. A thermostable anion-pillared metal-organic framework for C_2H_2/C_2H_4 and C_2H_2/CO_2 separations. *Chem. Eng. J.* **2018**, *352*, 803-810.

[25] Forrest, K. A.; Pham, T.; Chen, K.-J.; Jiang, X.; Madden, D. G.; Franz, D. M.; Hogan, A.; Zaworotko, M. J.; Space, B. Tuning the Selectivity between C_2H_2 and CO_2 in Molecular Porous Materials. *Langmuir*. **2021**, *37*, 13838-13845.

[26] Mukherjee, S.; Kumar, N.; Bezrukov, A. A.; Tan, K.; Pham, T.; Forrest, K. A.; Oyekan, K. A.; Qazvini, O. T.; Madden, D. G.; Space, B.; Zaworotko, M. J. Amino-Functionalised Hybrid Ultramicroporous Materials that Enable Single-Step Ethylene Purification from a Ternary Mixture. *Angew. Chem. Int. Ed.* **2021**, *60*, 10902-10909.

[27] Fan, W.; Wang, X.; Liu, X.; Xu, B.; Zhang, X.; Wang, W.; Wang, X.; Wang, Y.; Dai, F.; Yuan, D.; Sun, D. Regulating C_2H_2 and CO_2 Storage and Separation through Pore Environment Modification in a Microporous Ni-MOF. *ACS Sustain. Chem. Eng.* **2019**, *7*, 2134-2140.

[28] Qazvini, O. T.; Macreadie, L. K.; Telfer, S. G. Effect of Ligand Functionalization on the Separation of Small Hydrocarbons and CO_2 by a Series of MUF-15 Analogues. *Chem. Mater.* **2020**, *32*, 6744-6752.

[29] Qazvini, O. T.; Babarao, R.; Telfer, S. G. Multipurpose Metal-Organic Framework for the Adsorption of Acetylene: Ethylene Purification and Carbon Dioxide Removal. *Chem. Mater*. **2019**, *31*, 4919-4926.

[30] Mukherjee, S.; He, Y.; Franz, D.; Wang, S.-Q.; Xian, W.-R.; Bezrukov, A. A.; Space, B.; Xu, Z..; He, J.; Zaworotko, M. J. Halogen-C_2H_2 Binding in Ultramicroporous Metal-Organic Frameworks (MOFs) for Benchmark C_2H_2/CO_2 Separation Selectivity. *Chem.Eur.J.* **2020**, *26*, 4923-4929.

[31] Pei, J.; Wen, H.-M.; Gu, X.-W.; Qian, Q.-L.; Yang, Y.; Cui, Y.; Li, B.; Chen, B. L.; Qian, G. D. Dense Packing of Acetylene in a Stable and Low-Cost Metal-Organic Framework for Efficient C_2H_2/CO_2 Separation. *Angew.Chem.Int.Ed.* **2021**, *60,* 25068-25074.

[32] Zhang, X.; Lin, R.-B.; Wu, H.; Huang, Y.; Ye, Y.; Duan, J.; Zhou, W.; Li, J.-R.; Chen, B. Maximizing acetylene packing density for highly efficient C_2H_2/CO_2 separation through immobilization of amine sites within a prototype MOF. *Chem. Eng. J*. **2022**, *431*,134184.

[33] Ye, Y.; Xian, S.; Cui, H.; Tan, K.; Gong, L .; Liang, B.; Pham, T.; Pandey, H.; Krishna, R.; Lan, P. C.; Forrest, K. A.; Space, B.; Thonhauser, T.; Li, J.; Ma, S. Q. Metal-Organic Framework Based Hydrogen-Bonding Nanotrap for Efficient Acetylene Storage and Separation. *J. Am. Chem. Soc.* **2022**, *144*, 1681-1689.

[34] Gong, W.; Cui, H.; Xie, Y.; Li, Y.; Tang, X.; Liu, Y.; Cui, Y.; Chen. B. Efficient C_2H_2/CO_2 Separation in Ultramicroporous Metal-Organic Frameworks with Record C_2H_2 Storage Density. *J. Am. Chem. Soc*. **2021**, *143*, 14869−14876.

[35] Fan, S.-C.; Li, Y.-T.; Wang, Y.; Wang, J.-W.; Xue, Y.-Y.; Li, H.-P.; Li, S.-N.; Zhai, Q.-G. Amide-Functionalized Metal-Organic Frameworks Coupled with Open Fe/Sc Sites for Efficient Acetylene Purification. *Inorg. Chem.* **2021**, *60*, 18473-18482.

[36] Li, Y.-P.; Wang, Y.; Xue, Y.-Y.; Li, H.-P.; Zhai, Q.-G.; Li, S.-N.; Jiang, Y.-C.; Hu, M.-C.; Bu, X. Ultramicroporous Building Units as a Path to Bi-microporous Metal-Organic Frameworks with High Acetylene Storage and Separation Performance. *Angew. Chem. Int. Ed*. **2019**, *58*, 13590-13595.

[37] Li, Y.-T.; Zhang, J.-W.; Lv, H.-J.; Hu, M.-C.; Li, S.-N.; Jiang, Y.-C.; Zhai, Q.-G. Tailoring the Pore Environment of a Robust Ga-MOF by Deformed $[Ga_3O(COO)_6]$ Cluster for Boosting C_2H_2 Uptake and Separation. *Inorg. Chem*. **2020**, *59*, 10368-10373.

[38] Zhang, J.-W.; Hu, M.-C.; Li, S.-N.; Jiang, Y.-C.; Qu, P.; Zhai, Q.-G. Assembly of $[Cu_2(COO)_4]$ and $[M_3(\mu_3\text{-}O)(COO)_6]$(M = Sc, Fe, Ga, and In) building blocks into porous frameworks towards ultra-high C_2H_2/CO_2 and C_2H_2/CH_4 separation performance. *Chem. Commun*. **2018**, *54*, 2012-2015.

[39] Lv, H.-J.; Li, Y.-P.; Xue, Y.-Y.; Jiang, Y.-C.; Li, S.-N.; Hu, M.-C.; Zhai, Q.-G. Systematic Regulation of C_2H_2/CO_2 Separation by 3p-Block Open Metal Sites in a Robust Metal-Organic Framework Platform. *Inorg. Chem*. **2020**, *59*, 4825-4834.

[40] Duan, X.; Zhang, Q.; Cai, J.; Yang, Y.; Cui, Y.; He, Y.; Wu, C.; Krishna, R.; Chen. B.; Qian, G. A new metal-organic framework with potential for adsorptive separation of methane from carbon dioxide, acetylene, ethylene, and ethane established by simulated breakthrough experiments. *J. Mater. Chem. A*. **2014**, *2*, 2628-2633.

[41] Pei, J.; Shao, K.; Wang, J.-X.; Wen, H.-M.; Yang, Y.; Cui, Y. J.; Krishna, R.; Li, B.; Qian, G. A Chemically Stable Hofmann-Type Metal-Organic Framework with Sandwich-Like Binding Sites for Benchmark Acetylene Capture. *Adv. Mater*. **2020**, *32*, 1908275.

[42] Zhang, L.; Zou, C.; Zhao, M.; Jiang, K.; Lin, R.; He, Y.; Wu, C.-D.; Cui, Y..; Chen, B.; Qian, G. Doubly Interpenetrated Metal-Organic Framework for Highly Selective C_2H_2/CH_4 and C_2H_2/CO_2 Separation at Room Temperature. *Cryst. Growth Des*. **2016**, *16*, 7194-7197.

[43] Wen, H.-M.; Liao, C.; Li, L.; Yang, L.; Wang, J.; Huang, L.; Li, B.; Chen, B.; Hu, J. Reversing C_2H_2-CO_2 adsorption selectivity in an ultramicroporous metal-organic framework platform. *Chem. Commun*. **2019**, *55*, 11354-11357.

[44] Reynolds, J. E.; Walsh, K. M.; Li, B.; Kunal, P.; Chen, B.; Humphrey, S. M. Highly selective room temperature acetylene sorption by an unusual triacetylenic phosphine MOF. *Chem. Commun*. **2018**, *54*, 9937-9940.

[45] Fu, X.-P.; Wang, Y.-L.; Zhang, X.-F.; Krishna, R.; He, C.-T.; Liu, Q.-Y.; Chen, B. Collaborative pore partition and pore surface fluorination within a metal-organic framework for high-performance C_2H_2/CO_2 separation. *Chem. Eng. J*. **2022**, *432*, 134433.

[46] Li, Q.; Wu, N.; Li, J.; Wu, D. A Highly Connected Trinuclear Cluster Based Metal-Organic Framework for Efficient Separation of C_2H_2/C_2H_4 and C_2H_2/CO_2. *Inorg. Chem*. **2020**, *59*, 13005-13008.

[47] Zhao, J.; Li, Q.; Zhu, X.-C.; Li, J.; Wu, D. Highly Robust Tetranuclear Cobalt-Based 3D Framework for Efficient C_2H_2/CO_2 and C_2H_2/C_2H_4 Separations. *Inorg. Chem.* **2020**, *59*, 14424−14431.

[48] Liu, L.; Yao, Z.; Ye, Y.; Yang, Y.; Lin, Q.; Zhang, Z.; O'Keeffe, M.; Xiang, S. Integrating the Pillared-Layer Strategy and Pore-Space Partition Method to Construct Multicomponent MOFs for C_2H_2/CO_2 Separation. *J. Am. Chem. Soc*. **2020**, *142*, 9258-9266.

[49] Ye, Y.; Chen, S.; Chen, L.; Huang, J.; Ma, Z.; Li, Z.; Yao, Z.; Zhang, J.; Zhang, Z.; Xiang, S. Additive-Induced Supramolecular Isomerism and Enhancement of Robustness in Co(II)-Based MOFs for Efficiently Trapping Acetylene from Acetylene-Containing Mixtures. *ACS Appl. Mater. Interfaces.* **2018**, *10*, 30912-30918.

[50] Ye, Y.; Ma, Z.; Lin, R.-B.; Krishna. R.; Zhou, W.; Lin, Q.; Zhang, Z.; Xiang, S. ; Chen, B. Pore Space Partition within a Metal-Organic Framework for Highly Efficient C_2H_2/CO_2 Separation. *J. Am. Chem. Soc.* **2019**, *141*, 4130-4136.

[51] Zhang, L.; Jiang, K.; Li, Y.; Zhao, D.; Yang, Y.; Cui, Y.; Chen, B.; Qian, G. Microporous Metal-Organic Framework with Exposed Amino Functional Group for High Acetylene Storage and Excellent C_2H_2/CO_2 and C_2H_2/CH_4 Separations. *Cryst. Growth Des*. **2017**, *17*, 2319-2322.

[52] Zhang, L.; Jiang, K.; Yang, L.; Li, L.; Hu, E.; Yang, L.; Shao, K.; Xing, H.; Cui, Y.; Yang, Y.; Li, B.; Chen, B.; Qian, G. Benchmark C_2H_2/CO_2 Separation in an Ultra-Microporous Metal-Organic Framework via Copper(I)-Alkynyl Chemistry. *Angew. Chem. Int. Ed.* **2021**, *60*, 15995-16002.

[53] Meng, L.; Yang, L.; Chen, C.; Dong, X.; Ren, S.; Li, G.; Li, Y.; Han, Y.; Shi, Z.; Feng, S. Selective Acetylene Adsorption within an Imino-Functionalized Nanocage-Based Metal-Organic Framework. *ACS Appl. Mater. Interfaces*. **2020**, *12*, 5999-6006.

[54] Gao, J.; Qian, X.; Lin, R.-B.; Krishna, R.; Wu, H.; Zhou, W.; Chen, B. Mixed Metal-Organic Framework with Multiple Binding Sites for Efficient C_2H_2/CO_2 Separation. *Angew. Chem. Int. Ed*. **2020**, *59*, 4396-4400.

[55] Peng, Y.-L.; Pham, T.; Li, P.; Wang, T.; Chen, Y.; Chen, K.-J.; Forrest, K. A. Space, B.; Cheng, P.; Zaworotko, M. J.; Zhang, Z. Robust Ultramicroporous Metal-Organic Frameworks with Benchmark Affinity for Acetylene. *Angew. Chem. Int. Ed*. **2018**, *57*, 10971-10975.

[56] Sharma, S.; Mukherjee, S.; Desai, A. V. Vandichel, M.; Dam, G. K.; Jadhav, A.; Kociok-Köhn, G..; Zaworotko, M. J.; Ghosh, S. K. Efficient Capture of Trace Acetylene by an Ultramicroporous Metal-Organic Framework with Purine Binding Sites. *Chem. Mater*. **2021**, *33*, 5800-5808.

[57] Scott, H. S.; Shivanna, M.; Bajpai, A.; Madden, D. G.; Chen, K.-J.; Pham, T.;Forrest, K. A.; Hogan, A.; Space, B.; Perry, J. J.; Zaworotko, M. J. Highly Selective Separation of C_2H_2 from CO_2 by a New DichromateBased Hybrid Ultramicroporous Material. *ACS Appl. Mater. Interfaces*. **2017**, *9*, 33395-33400.

[58] Yang, H.; Trieu, T. X.; Zhao, X.; Wang, Y.; Wang, Y.; Feng, P.; Bu, X. Lock-and-Key and Shape-Memory Effects in an Unconventional Synthetic Path to Magnesium Metal-Organic Frameworks. *Angew. Chem. Int. Ed*. **2019**, *58*, 11757-11762.

[59] Zhang, L.; Jiang, K.; Zhang, J.; Pei, J.; Shao, K.; Cui, Y.; Yang, Y.; Li, B.; Chen, B.; Qian, G. Low-Cost and High-Performance Microporous Metal-Organic Framework for Separation of Acetylene from Carbon Dioxide. *ACS Sustainable Chem. Eng*. **2019**, *7*, 1667-1672.

[60] Liu, S.; Huang, Y.; Dong, Q.; Wang, H.; Duan, J. Finely Tuned Framework Isomers for Highly Efficient C_2H_2 and CO_2 Separation. *Inorg. Chem*. **2020**, *59*, 9569-9578.

[61] Dong, Q.; Guo, Y.; Cao, H.; Wang, S.; Matsuda, R.; Duan. J. Accelerated C_2H_2/CO_2 Separation by a Se-Functionalized Porous Coordination Polymer with Low Binding Energy. *ACS Appl. Mater. Interfaces*. **2020**, *12*, 3764−3772.

[62] Chen, S.; Behera, N.; Yang, C.; Dong, Q.; Zheng, B.; Li, Y.; Tang, Q.; Wang, Z. ; Wang, Y.; Duan, J. A chemically stable nanoporous coordination polymer with fixed and free Cu^{2+} ions for boosted C_2H_2/CO_2 separation. *Nano Res*. **2021**, *14*, 546-553.

[63] Li, P.; He, Y.; Zhao, Y.; Weng, L.; Wang, H.; Krishna, R.; Wu, H.; Zhou, W.; O'Keeffe, M.; Han, Y.; Chen, B. A Rod-Packing Microporous Hydrogen-Bonded Organic Framework for Highly Selective Separation of C_2H_2/CO_2 at Room Temperature. *Angew. Chem*. **2015**, *127*, 584-587.

[64] Li, Y.-Z.; Wang, G.-D.; Ma, L.-N.; Hou, L.; Wang, Y.-Y.; Zhu, Z. Multiple Functions of Gas Separation and Vapor Adsorption in a New MOF with Open Tubular Channels. *ACS Appl. Mater. Interfaces.* **2021**, *13*, 4102-4109.

[65] Wang, G.-D.; Wang, H.-H.; Shi, W.-J.; Hou, L.; Wang, Y.-Y.; Zhu, Z. A highly stable MOF with F and N accessible sites for efficient capture and separation of acetylene from ternary mixtures. *J. Mater. Chem. A*. **2021**, *9*, 24495-24502.

[66] Xiang, S.-C.; Zhang, Z.; Zhao, C.-G.; Hong, K.; Zhao, X.; Ding, D.-R.; Xie, M.-H.; Wu, C.-D.; Das, M. C.; Gill, R.; Thomas, K. M.; Chen, B. Rationally tuned micropores within enantiopure metal-organic frameworks for highly selective separation of acetylene and ethylene. *Nat. Commun*. **2011**, DOI: 10.1038/ncomms1206.

[67] Li, H.; Bonduris, H.; Zhang, X.; Ye, Y.; Alsalme, A.; Lin, R.-B.; Zhang, Z.; Xiang, S.; Chen, B. A microporous metal-organic framework with basic sites for efficient C_2H_2/CO_2 separation. *J. Solid State Chem*. **2020**, *284*, 121209.

[68] Zeng, H.; Xie, M.; Huang, Y.-L.; Zhao, Y.; Xie, X.-J.; Bai, J.-P.; Wan, M.-Y.; Krishna, R.; Lu, W.; Li, D. Induced Fit of C_2H_2 in a Flexible MOF Through Cooperative Action of Open Metal Sites. *Angew. Chem. Int. Ed*. **2019**, *58*, 8515-8519.

[69] Fan, W.; Yuan, S.; Wang, W.; Feng, L.; Liu, X.; Zhang, X.; Wang, X.; Kang, Z.; Dai, F.; Yuan, D.; Sun, D.; Zhou, H.-C. Optimizing Multivariate Metal-Organic Frameworks for Efficient C_2H_2/CO_2 Separation. *J. Am. Chem. Soc*. **2020**, *142*, 8728-8737.

[70] Li, T.; Cui, P.; Sun, D. Uncoordinated Hexafluorosilicates in a Microporous Metal-Organic Framework Enabled C_2H_2/CO_2 Separation. *Inorg. Chem*. **2022**, *61*, 4251-4256.

[71] Forrest, K. A.; Pham, T.; Chen, K.-J.; Jiang, X.; Madden, D. G.; Franz, D. M.; Hogan, A.; Zaworotko, M. J.; Space, B. Tuning the Selectivity between C_2H_2 and CO_2 in Molecular Porous Materials. *Langmuir*. **2021**, *37*, 13838-13845.

[72] Wang, G.-D.; Li, Y.-Z.; Zhang, W.-F.; Hou, L.; Wang, Y.-Y.; Zhu, Z. Acetylene Separation by a Ca-MOF Containing Accessible Sites of Open Metal Centers and Organic Groups. *ACS Appl. Mater. Interfaces*. **2021**, *13*, 58862-58870.

[73] Cui, H.; Ye, Y.; Arman, H.; Li, Z.; Alsalme, A.; Lin, R.-B.; Chen, B. Microporous Copper Isophthalate Framework of mot Topology for C_2H_2/CO_2 Separation. *Cryst. Growth Des*. **2019**, *19*, 5829-5835.

[74] Liu, R.; Liu, Q.-Y.; Krishna, R.; Wang, W.; He, C.-T.; Wang, Y.-L. Water-Stable Europium 1,3,6,8-Tetrakis(4-carboxylphenyl)pyrene Framework for Efficient C_2H_2/CO_2 Separation. *Inorg. Chem*. **2019**, *58*, 5089-5095.

[75] Niu, Z.; Cui, X..; Pham, T.; Verma, G.; Lan, P.; Shan, C.; Xing, H.; Forrest, K. A.; Suepaul, S.; Space, B.; Nafady, A.; Al-Enizi, A. M.; Ma, S. A MOF-based Ultra-Strong Acetylene Nano-trap for Highly Efficient C_2H_2/CO_2 Separation. *Angew. Chem. Int. Ed*. **2021**, *60*, 5283-5288.

[76] Yao, Z.; Zhang, Z.; Liu, L.; Li, Z.; Zhou, W.; Zhao, Y.; Han, Y.; Chen, B.; Krishna, R.; Xiang, S. Extraordinary Separation of Acetylene-Containing Mixtures with Microporous Metal-Organic Frameworks with Open O Donor Sites and Tunable Robustness through Control of the Helical Chain Secondary Building Units. *Chem. Eur. J*. **2016**, *22*, 5676-5683.

[77] Liu, L.; Yao, Z.; Ye, Y.; Chen, L.; Lin, Q.; Yang, Y.; Zhang, Z.; Xiang, S. Robustness, Selective Gas Separation, and Nitrobenzene Sensing on Two Isomers of Cadmium Metal-Organic Frameworks Containing Various Metal-O-Metal Chains. *Inorg. Chem*. **2018**, *57*, 12961-12968.

[78] Zhang, L.; Jiang, K.; Li, Y.; Zhao, D.; Yang, Y.; Cui, Y.; Chen, B.; Qian, G. Microporous Metal-Organic Framework with Exposed Amino Functional Group for High Acetylene Storage and Excellent C_2H_2/CO_2 and C_2H_2/CH_4 Separations. *Cryst. Growth Des*. **2017**, *17*, 2319-2322.

[79] Xu, T.; Jiang, Z.; Liu, P.; Chen, H.; Lan, X.; Chen, D.; Li, L.; He, Y. Immobilization of Oxygen Atoms in the Pores of Microporous Metal-Organic Frameworks for C_2H_2 Separation and Purification. *ACS Appl. Nano Mater*. **2020**, *3*, 2911-2919.

[80] Du, Y.; Chen, Y.; Wang, Y.; He, C.; Yang, J.; Li, L.; Li, J. Optimized pore environment for efficient high selective C_2H_2/C_2H_4 and C_2H_2/CO_2 separation in a metal-organic framework. *Sep. Purif. Technol*. **2021**, *256*, 117749.

[81] Xu, N.; Jiang, Y.; Sun, W.; Li, J. H.; Wang, L.; Jin, Y.; Zhang, Y.; Wang, D.; Duttwyler, S. Gram-Scale Synthesis of an Ultrastable Microporous Metal-Organic Framework for Efficient Adsorptive Separation of C_2H_2/CO_2 and C_2H_2/CH_4. *Molecules*. **2021**, *26*, 5121.

[82] Zhang, J.-P.; Chen, X.-M. Optimized Acetylene/Carbon Dioxide Sorption in a Dynamic Porous Crystal. *J. Am. Chem. Soc*. **2009**, *131*, 5516-5521.

[83] Sanii, R.; Hua, C.; Patyk-Kaz´mierczak, E.; Zaworotko, M. J. Solvent-directed control over the topology of entanglement in square lattice (sql) coordination networks. *Chem. Commun*. **2019**, *55*, 1454-1457.

Table S5 Comparison of the reported materials on C_2H_2/C_2H_4 adsorption capacity, C_2H_2/C_2H_4 adsorption enthalpy (Q_{st}) and IAST selectivity towards C_2H_2/C_2H_4

Adsorbents	Surface area ($m^2 \cdot g^{-1}$, BET)	C_2H_2 uptake ($cm^3 \cdot g^{-1}$)	C_2H_4 uptake ($cm^3 \cdot g^{-1}$)	IAST (C_2H_2/C_2H_4) (50/50)	Qst (C_2H_2 kJ·mol^{-1})	Qst (C_2H_4 kJ·mol^{-1})	Ref
ZNU-5	751.5	128.6	11.9	255	27.8	-	This work
ZNU-4	358.6	85.1	39.9	11.8	50.3	31.4	This work
CPL-5[a]	523	67.4	41.2	6	31.3	19.1	[1]
CPL-1[a]	414	46.4	6.94	26.8	40.2	36.3	[1]
CPL-2[a]	495	70.1	41.7	12	30.8	20.3	[1]
NbU-1	368.2	62.0	45.0	5.9	38.3	37.9	[2]
$[Cu_2(TPPB)_2](DMF)_8$a	216	44.0	4.80	18.4	34.1	13.2	[3]
M'MOF-4a[b]	602	~32.0	~9.50	14.3	35.2	-	[4]
M'MOF-5a[b]	202	~31.0	~12.0	4.9	50.1	-	[4]
M'MOF-6a[b]	369	~39.5	~15.0	7.4	30.3	-	[4]
M'MOF-7a[b]	90	~18.0	~6.0	7.4	47.1	-	[4]
BSF-1	535	52.6	36.6	2.3	31	26	[5]
BSF-2	403	41.4	29.6	2.9	37.7	23.5	[6]
BSF-3-Co	437	86.2	56.2	10.2	-	-	[7]
BSF-3	458	80.4	53.1	8.0	42.7	27.4	[7]
BSF-4	437	53.3	34.9	7.3	35	-	[8]
BSF-9	532	76.3	37.1	41.4	54	35	[9]
HUST-5[c]	802.2	~50.0	~38.0	1.8	30.6	29.2	[10]
HUST-6[c]	645.3	~80.0	~50.0	3.8	31.1	30.2	[10]
NPU-1	1396	114.0	94.0	1.4	27.88	23.95	[11]
NPU-2	1580	90.0	77.2	1.25	20.98	18.18	[11]
NPU-3	1834	57.8	49.7	1.32	19.93	17.79	[11]
M'MOF-3a[d]	110.1	42.5	9.0	5.23	27.1	27.3	[12]
SNNU-95	206.6	15.1	15.3	1.7	47.2	35.1	[13]
MUF-17[d]	247	111.6	79.7	8.7	49.5	31.3	[14]
MgMOF-74[b]	927	141.0	69.4	2.2	41	-	[15]

NOTT-300	1370	142.0	95.9	2.3	32	16	[16]
SIFSIX-2-Cu-i	503	90.0	49.1	41.0	41.9	30.7	[17]
TIFSIX-2-Ni-i	480.5	94.3	54.2	16.3	40	31	[18]
JCM-1	550	75.0	35.0	13.2	36.9	34.2	[19]
UTSA-100a	970	95.7	37.2	19.6	22	-	[20]
ELM-12	-	57.3	22.5	~28	25.4	-	[21]
SIFSIX-3-Zn	250	81.5	50.2	13.72	21	-	[22]
SIFSIX-3-Ni	368	73.9	39.2	5.98	30.5	-	[22]
FJU-22a	828.19	114.8	85.8	25.8	23	-	[23]
PCP-33	1248	121.8	86.8	~3	27.5	23.9	[24]

a : IAST(C_2H_2:C_2H_4)1:99

b : At temperature of 295K , IAST(C_2H_2:C_2H_4)1:99

c: At temperature of 273K , IAST(C_2H_2:C_2H_4)1:99

d: At temperature of 293K

References:

[1] Zheng, F.; Guo, L.; Gao, B.; Li, L.; Zhang, Z.; Yang, Q.; Yang, Y.; Su, B.; Ren, Q.; Bao, Z. Engineering the Pore Size of Pillared-Layer Coordination Polymers Enables Highly Efficient Adsorption Separation of Acetylene from Ethylene. *ACS Appl. Mater. Interfaces*. **2019**, *11*, 28197-28204.

[2] Li, J.; Jiang, L.; Chen, S.; Kirchon, A.; Li, B.; Li, Y.; Zhou, H.-C. Metal-Organic Framework Containing Planar Metal-Binding Sites: Efficiently and Cost-Effectively Enhancing the Kinetic Separation of C_2H_2/C_2H_4. *J. Am. Chem. Soc*. **2019**, *141*, 3807−3811.

[3] Chen, D.-M.; Liu, X.-H.; Zhang, J.-H.; Liu, C.-S. A flexible doubly interpenetrated metal-organic framework with gate opening effect for highly selective C_2H_2/C_2H_4 separation at room temperature. *CrystEngComm*. **2018**, *20*, 2341-2345.

[4] Das, M. C.; Guo, Q.; He, Y.; Kim, J.; Zhao, C.-G.; Hong, K.; Xiang, S.; Zhang, Z.; Thomas, K. M.; Krishna, R.; Chen, B. Interplay of Metalloligand and Organic Ligand to Tune Micropores within Isostructural Mixed-Metal Organic Frameworks (M′MOFs) for Their Highly Selective Separation of Chiral and Achiral Small Molecules. *J. Am. Chem. Soc*. **2012**, *134*, 8703−8710.

[5] Zhang, Y.; Yang, L.; Wang, L.; Duttwyler, S.; Xing, H. A Microporous Metal-Organic Framework Supramolecularly Assembled from a CuII Dodecaborate Cluster Complex for Selective Gas Separation. *Angew. Chem. Int. Ed*. **2019**, *58*, 8145–8150.

[6] Zhang, Y.; Yang, L.; Wang, L.; Cui, X.; Xing, H.; Pillar iodination in functional boron cage hybrid supramolecular frameworks for high performance separation of light hydrocarbons. *J. Mater. Chem. A*. **2019**, *7*, 27560-27566.

[7] Zhang, Y.; Hu, J.; Krishna, R.; Wang, L.; Yang, L.; Cui, X.; Duttwyler, S.; Xing, H. Rational Design of Microporous MOFs with Anionic Boron Cluster Functionality and Cooperative Dihydrogen Binding Sites for Highly Selective Capture of Acetylene. *Angew. Chem. Int. Ed*. **2020**, *59*, 17664–17669.

[8] Zhang, Y.; Wang, L.; Hu, J.; Duttwyler, S.; Cui, X.; Xing, H. Solvent-dependent supramolecular self-assembly of boron cage pillared metal-organic frameworks for selective gas separation. *CrystEngComm*. **2020**, *22*, 2649–2655.

[9] Sun, W.; Hu, J.; Duttwyler, S.; Wang, L.; Krishna, R.; Zhang, Y. Highly selective gas separation by two isostructural boron cluster pillared MOFs. *Sep. Purif. Technol*. **2022**, *283*, 120220.

[10] Yu, F.; Hu, B.-Q.; Wang, X.-N.; Zhao, Y.-M.; Li, J.-L.; Li, B.; Zhou, H.-C. Enhancing the separation efficiency of a C_2H_2/C_2H_4 mixture by a chromium metal–organic framework fabricated via post-synthetic metalation. *J. Mater. Chem. A*. **2020**, **8**, 2083–2089.

[11] Zhu, B.; Cao, J.-W.; Mukherjee, S.; Pham, T.; Zhang, T.; Wang, T.; Jiang, X.; Forrest, K. A.; Zaworotko, M. J.; Chen, K.-J. Pore Engineering for One-Step Ethylene Purification from a Three Component Hydrocarbon Mixture. *J. Am. Chem. Soc*. **2021**, *143*,1485−1492.

[12] Das, M. C.; Guo, Q.; He, Y..; Kim, J.; Zhao, C.-G.; Hong, K.; Xiang, S.; Zhang, Z.; Thomas, K. M.; Krishna, R.; Chen, B. Interplay of Metalloligand and Organic Ligand to Tune Micropores within Isostructural Mixed-Metal Organic Frameworks (M′MOFs) for Their Highly Selective Separation of Chiral and Achiral Small Molecules. *J. Am. Chem. Soc*. **2012**, *134*, 8703−8710.

[13] Li, H.; Li, S.; Hou, X.; Jiang, Y.; Hu, M.; Zhai, Q.-G. Enhanced gas separation performance of an ultramicroporous pillared-layer framework induced by hanging bare Lewis basic pyridine groups. *Dalton Trans*. **2018**, *47*, 9310-9316.

[14] Qazvini, O. T.; Babarao, R.; Telfer, S. G. Multipurpose Metal-Organic Framework for the Adsorption of Acetylene: Ethylene Purification and Carbon Dioxide Removal. *Chem. Mater*. **2019**, *31*, 4919-4926.

[15] He, Y.; Krishn, R.; Chen, B. Metal–organic frameworks with potential for energy-efficient adsorptive separation of light hydrocarbons. *Energy Environ. Sci*. **2012**, *5*, 9107–9120.

[16] Yang, S.; Ramirez-Cuesta, A. J.; Newby, R.; Garcia-Sakai, V.; Manuel, P.; Callear, S. K.; Campbell, S. I.; Tang, C. C.; Schröder, M. Supramolecular binding and separation of hydrocarbons within a functionalized porous metal–organic framework. *Nat. Chem*. **2015**, *7*, 121-129.

[17] Cui, X.; Chen, K.; Xing, H.; Yang, Q.; Krishna, R.; Bao, Z.; Wu, H.; Zhou, W.; Dong, X.; Han, Y.; Li, B.; Ren, Q.; Zaworotko, M. J.; Chen, B. Pore chemistry and size control in hybrid porous materials for acetylene capture from ethylene. *Science*. **2016**, *353*, 141–144.

[18] Jiang, M.; Cui, X.; Yang, L.; Yang, Q.; Zhang, Z.; Yang, Y.; Xing, H. A thermostable anion-pillared metal-organic framework for C_2H_2/C_2H_4 and C_2H_2/CO_2 separations. *Chem. Eng. J*. **2018**, *352*, 803-810.

[19] Lee, J.; Chuah, C. Y.; Kim, J.; Kim, Y.; Ko, N.; Seo, Y.; Kim, K.; Bae, T. H. ; Lee, E. Separation of Acetylene from Carbon Dioxide and Ethylene by a Water-Stable Microporous Metal-Organic Framework with Aligned Imidazolium Groups inside the Channels. *Angew. Chem. Int. Ed*. **2018**, *57*, 7869-7873.

[20] Hu, T.-L.; Wang, H.; Li, B.; Krishna, R.; Wu, H.; Zhou, W.; Zhao, Y.; Han, Y.; Wang, X.; Zhu, W.; Yao, Z.; Xiang, S.; Chen, B.; Microporous metal–organic framework with dual functionalities for highly efficient removal of acetylene from ethylene/acetylene mixtures. Nat. Commun. 2015, 6, 7328–7335.

[21] Li, L.; Lin, R.-B.; Krishna, R.; Wang, X.; Li, B.; Wu, H.; Li, J.; Zhou, W.; Chen, B. Efficient separation of ethylene from acetylene/ethylene mixtures by a flexible-robust metal–organic framework. *J. Mater. Chem. A*. **2017**, *5*, 18984-18988.

[22] Cui, X.; Chen, K.; Xing, H.; Yang, Q.; Krishna, R.; Bao, Z.; Wu, H.; Zhou, W.; Dong, X.; Han, Y.; Li, B.; Ren, Q.; Zaworotko, M. J.; Chen, B. Pore chemistry and sizecontrol in hybrid porous materials for acetylene capture from ethylene. *Science*. **2016**, *353*, 141–144.

[23] Yao, Z.; Zhang, Z.; Liu, L.; Z. Li, Zhou, W.; Zhao, Y.; Han, Y.; Chen, B.; Krishna, R.; Xiang, S. Extraordinary Separation of Acetylene-Containing Mixtures with Microporous Metal–Organic Frameworks with Open O Donor Sites and Tunable Robustness through Control of the Helical Chain Secondary Building Units. *Chem. Eur. J*. **2016**, *22*, 5676-5683.

[24] Duan, J.; Jin, W.; Krishna, R. Natural Gas Purification Using a Porous Coordination Polymer with Water and Chemical Stability. *Inorg. Chem*. **2015**, *54*, 4279-4284.

Table S6 Comparison of the reported materials on C_2H_2/CH_4 adsorption capacity,C_2H_2/CH_4 adsorption enthalpy (Q_{st}) and IAST selectivity towards C_2H_2/CH_4

Adsorbents	Surface area ($m^2 \cdot g^{-1}$,	C_2H_2 uptake ($cm^3 \cdot g^{-1}$)	CH_4 uptake ($cm^3 \cdot g^{-1}$)	IAST (C_2H_2/C_2H_4) (50/50)	Qst (C_2H_2 kJ· mol^{-1})	Qst (CH_4 kJ· mol^{-1})	Ref

	BET)						
ZNU-5	751.5	128.6	3.49	850	27.8	-	This work
ZNU-4	358.6	85.1	12.3	299	50.28	21.31	This work
SNNU-13	530.82	72.3	10.0	48.5	39.6	19.9	[1]
SNNU-14	514.59	71.0	9.70	93.5	45.8	12.7	[1]
SNNU-15	299.48	43.5	6.10	61.6	40.9	27.5	[1]
SNNU-16	421.3	46.0	12.1	100.7	52.6	16.7	[1]
FeNi-M'MOF	-	96.5	25.7	198.9	35.1	8	[2]
JLU-MOF66	471	54.6	9.50	86.2	35.6	21.2	[3]
JLU-MOF67	480	35.2	8.30	20	33	18.2	[3]
NbU-11[a]	550.6	77.3	14.7	175.8	31.9	21.5	[4]
UTSA-50[d]	604	90.6	18.8	68	39.4	18.6	[5]
SNNU-Bai67	1088.7	116.7	18.5	37.6	35.1	23.1	[6]
VNU-18	1180.4	101.5	19.0	53.8	30.7	19.7	[6]
FJI-C1	1726.3	93.8	9.70	39.3	28.9	11.4	[7]
NbU-5	671	92.0	68.0	52.9	32.1	20.6	[8]
SNNU-64	463.8	58.6	9.80	35.8	34.6	19.2	[9]
NKMOF-1-Ni	382	61.0	22.2	>1000	60.3	28.5	[10]
Cu-TDPAT	-	178.0	28.3	127.1	42.5	20.7	[11]
SNNU-65-Cu-Ga	1918	141.6	13.6	120.6	31.7	15.2	[12]
SNNU-65-Cu-In	1936.2	153.3	13.8	69.5	23.4	15.8	[12]
Y-H3TDPAT	962	100.0	17.5	77.2	38.2	13.5	[13]
BUT-70A	460	69.5	9.70	66.6	23.9	15	[14]
FJI-C4	690	72.5	18.4	51	27	20.8	[15]
BSF-1	535	52.6	10.5	46.9	31	-	[16]
BSF-2	403	41.5	5.40	324	37.7	23.5	[17]
BSF-3	458	80.4	13.4	205	42.7	-	[18]
FIR-51[b]	918.6	141.9	19.0	39.6	24.5	12.7	[19]
FJU-36a[d]	409	52.2	10.5	17.7	32.9	16.9	[20]

ZJNU-69	1655	171.7	19.8	34.5	31.2	15.9	[21]
Fe2(dobdc) [c]	1350	154.3	17.2	700	47	20	[22]

a: At temperature of 295K

b: At temperature of 294K

c: At temperature of 318K

d: At temperature of 296K

References:

[1] Li, H.-P.; Dou, Z.-D.; Wang, Y.; Xue, Y. Y.; Li, Y. P.; Hu, M.-C.; Li, S.-N.; Jiang, Y.-C.; Zhai, Q.-G. Tuning the Pore Surface of an Ultramicroporous Framework for Enhanced Methane and Acetylene Purification Performance. *Inorg. Chem*. **2020**, *59*, 16725-16736.

[2] Zheng, Y.; Yong, J.; Zhu, Z. W.; Chen, J. Z.; Song, Z. Y.; Gao, J. K. Spin crossover in metal–organic framework for improved separation of C_2H_2/CH_4 at room temperature. *J. Solid State Chem*. **2021**, *304*, 122554.

[3] Kan, L. Li, G.; Liu, Y. Highly Selective Separation of C_3H_8 and C_2H_2 from CH_4 within Two Water-Stable Zn_5 Cluster-Based Metal−Organic Frameworks. *ACS Appl. Mater. Interfaces*. **2020**, *12*, 18642−18649.

[4] Wu, N.; Li, Q.; Li, J.; Wu, D.; Li, Y. 4- Connected Cobalt-Based 3D Framework with a High Affinity for Acetylene. *Inorg. Chem*. **2020**, *59*, 9461-9464.

[5] Xu, H.; He, Y.; Zhang, Z.; Xiang, S.; Cai, J.; Cui, Y.; Yang, Y.; Qian, G.; Chen, B. A microporous metal-organic framework with both open metal and Lewis basic pyridyl sites for highly selective C_2H_2/CH_4 and C_2H_2/CO_2 gas separation at room temperature. *J. Mater. Chem. A*. **2013**, *1*, 77-81.

[6] Cheng, H.; Wang, Q.; Ding, M.; Gao, Y.; Xue, D.; Bai, J. Modifying a partial corn-sql layer-based (3,3,3,3,4,4)-c topological MOF by substitution of OH− with Cl− and its highly selective adsorption of C2 hydrocarbons over CH_4. *Dalton Trans*. **2021**, *50*, 4840-4847.

[7] Huang, Y.; Lin, Z.; Fu, H.; Wang, F.; Shen, M.; Wang, X.; Cao, R. Porous Anionic Indium-Organic Framework with Enhanced Gas and Vapor Adsorption and Separation Ability. *ChemSusChem*. **2014**, *7*, 2647-2653.

[8] Li, J.; Chen, S.; Jiang, L.; Wu, D.; Li, Y. Pore Space Partitioning of Metal-Organic Framework for C_2Hx Separation from Methane. *Inorg. Chem*. **2019**, *58*, 5410-5413.

[9] Zhang, J.-W.; Qu, P.; Hu, M.-C.; Li, S.-N.; Jiang, Y.-C.; Zhai, Q.-G. Self-Assembly of a Rare Nanocage-based Fe-MOF toward High Methane Purification Performance. *Cryst. Growth Des*. **2020**, *20*, 5657-5663.

[10] Peng, Y.-L.; Pham, T.; Li, P.; Wang, T.; Chen, Y.; Chen, K.-J.; Forrest, K. A.; Space, B.; Cheng, P.; Zaworotko, M. J.; Zhang, Z. Robust Ultramicroporous Metal-Organic Frameworks with Benchmark Affinity for Acetylene. *Angew. Chem. Int. Ed*. **2018**, *57*, 10971-10975.

[11] Liu, K.; Ma, D.; Li, B.; Li, Y.; Yao, K.; Zhang, Z.; Han, Y.; Shi, Z. High storage capacity and separation selectivity for C_2 hydrocarbons over methane in the metal-organic framework Cu–TDPAT. *J. Mater. Chem. A*. **2014**, *2*, 15823–15828.

[12] Zhang, J. W.; Hu, M. C.; Li, S. N.; Jiang, Y. C.; Qu, P.; Zhai, Q. G. Assembly of $[Cu_2(COO)_4]$ and $[M_3(l_3\text{-}O)(COO)_6]$ (M = Sc, Fe, Ga, and In) building blocks into porous frameworks towards ultra-high C_2H_2/CO_2 and C_2H_2/CH_4 separation performance. *Chem. Commun.* **2018**, *54*, 2012-2015.

[13] Liu, K.; Li, X.; Ma, D.; Han, Y.; Li, B.; Shi, Z.; Li, Z.; Wang, L. A microporous yttrium metal-organic framework of an unusual nia topology for high adsorption selectivity of C_2H_2 and CO_2 over CH_4 at room temperature. *Mater. Chem. Front*. **2017**, *1*, 1982-1988.

[14] Guo, Z.-J.; Yu, J.; Zhang, Y.-Z.; Zhang, J.; Chen, Y.; Wu, Y.; Xie, L.-H.; Li, J.-R. Water-Stable In(III)-Based Metal−Organic Frameworks with RodShaped Secondary Building Units: Single-Crystal to Single-Crystal Transformation and Selective Sorption of C_2H_2 over CO_2 and CH_4. *Inorg. Chem*. **2017**, *56*, 2188-2197.

[15] Li, L.; Wang, X.; Liang, J.; Huang, Y.; Li, H.; Lin, Z.; Cao, R. Water-Stable Anionic Metal−Organic Framework for Highly Selective Separation of Methane from Natural Gas and Pyrolysis Gas. *ACS Appl. Mater. Interfaces*. **2016**, *8*, 9777-9781.

[16] Zhang, Y.; Yang, L.; Wang, L.; Duttwyler, S.; Xing, H. A Microporous Metal-Organic Framework Supramolecularly Assembled from a CuII Dodecaborate Cluster Complex for Selective Gas Separation. *Angew. Chem. Int. Ed*. **2019**, *58*, 8145–8150.

[17] Zhang, Y.; Yang, L.; Wang, L.; Cui, X.; Xing, H. Pillar iodination in functional boron cage hybrid supramolecular frameworks for high performance separation of light hydrocarbons. *J. Mater. Chem. A*. **2019**, *7*, 27560-27566.

[18] Zhang, Y.; Hu, J.; Krishna, R.; Wang, L.; Yang, L.; Cui, X.; Duttwyler, S.; Xing, H. B. Rational Design of Microporous MOFs with Anionic Boron Cluster Functionality and Cooperative Dihydrogen Binding Sites for Highly Selective Capture of Acetylene. *Angew. Chem. Int. Ed*. **2020**, *59*, 17664-17669.

[19] Fu, H.-R.; Wang, F.; Zhang, J. A stable zinc-4-carboxypyrazole framework with high uptake and selectivity of light hydrocarbons. *Dalton Trans*. **2015**, *44*, 2893-2896.

[20] Liu, L.; Yao, Z..; Ye, Y.; Chen, L.; Lin, Q.; Yang, Y.; Zhang, Z.; Xiang, S. Robustness, Selective Gas Separation, and Nitrobenzene Sensing on Two Isomers of Cadmium Metal−Organic Frameworks Containing Various Metal-O-Metal Chains. *Inorg. Chem*. **2018**, *57*, 12961−12968.

[21] Chen, F.; Wang, Y.; Bai, D.; He, M.; Gao, X.; He, Y. Selective adsorption of C_2H_2 and CO_2 from CH_4 in an isoreticular series of MOFs constructed from unsymmetrical diisophthalate linkers and the effect of alkoxy group functionalization on gas adsorption. *J. Mater. Chem. A*. **2018**, *6*, 3471-3478.

[22] Bloch, E. D.; Queen, W. L.; Krishna, R.; Zadrozny, J. M.; Brown, C. M. Long, J. R. Hydrocarbon Separations in a Metal-Organic Framework with Open Iron(II) Coordination Sites. *Science*. **2012**, *30*, 1606-1610.